OCEAN DRILLING PROGRAM

LEG 159 PRELIMINARY REPORT

THE CÔTE D'IVOIRE-GHANA TRANSFORM MARGIN EASTERN EQUATORIAL ATLANTIC

Dr. Jean Mascle
Co-Chief Scientist, Leg 159
Laboratoire de Géodynamique Sous Marine
B.P. 48
06230 Villefranche-sur-Mer
France

Dr. G.P. Lohmann
Co-Chief Scientist, Leg 159
Woods Hole Oceanographic Institution
Woods Hole, MA 02543
U.S.A.

Dr. Peter Clift
Staff Scientist, Leg 159
Ocean Drilling Program
Texas A&M University Research Park
1000 Discovery Drive
College Station, TX 77845-9547
U.S.A.

Timothy J.G. Francis
Acting Director
ODP/TAMU

Jack Baldauf
Acting Deputy Director &
Manager, Science Operations
ODP/TAMU

April 1995

Preliminary Report No. 59

First Printing 1995

Distribution

Copies of this publication may be obtained from the Director, Ocean Drilling Program, Texas A&M University Research Park, 1000 Discovery Drive, College Station, Texas 77845-9547, U.S.A.
In some cases, orders for copies may require payment for postage and handling.

D I S C L A I M E R

SCIENTIFIC REPORT

The following scientists were aboard *JOIDES Resolution* for Leg 159 of the Ocean Drilling Program:

Jean Mascle, Co-Chief Scientist (Laboratoire de Géodynamique Sous Marine, B.P. 4806230 Villefranche-sur-Mer, France; E-mail: mascle@ccrv.obs-vlfr.fr)

G.P. Lohmann, Co-Chief Scientist (Woods Hole Oceanographic Institution, Woods Hole, Massachusetts 02543, U.S.A.; E-mail: glohmann@whoi.edu)

Peter Clift, Staff Scientist (Ocean Drilling Program, 1000 Discovery Drive, Texas A&M University Research Park, College Station, Texas 77845-9547, U.S.A.; E-mail: clift@nelson.tamu.edu)

Thomas Akamaluk, Science Observer (Geological Survey Department, P.O. Box M80, Accra, Ghana)

William Simon Allerton, Paleomagnetist (Department of Earth Sciences, University of Oxford, Parks Road, Oxford OX1 3PR, United Kingdom; E-mail: simona@earth.ox.ac.uk)

Maria Vera Susanna Ask, Physical Properties Specialist (Engineering Geology, Royal Institute of Technology, S-100 44 Stockholm, Sweden; E-mail: ask@ce.kth.se)

Enriqueta C. Barrera, Inorganic Geochemist (Department of Geological Sciences, University of Michigan, Ann Arbor, Michigan 48109-1063, U.S.A.; E-mail: ebarrera@um.cc.umich.edu)

Eric Barton, Petroleum Geologist/Organic Geochemist (801 LaFarge Avenue, Louisville, Colorado 80027, U.S.A.)

Christophe Basile, JOIDES Logging Scientist (Institut Dolomieu, Université Joseph Fourier, 15 rue Maurice Gignoux, 38031 Grenoble Cedex, France)

Jean-Pierre Bellier, Paleontologist (foraminifers) (Département de Géologie Sédimentaire, Université Pierre et Marie Curie, Paris 6, T15-4E, 4 place Jussieu, 75252 Paris Cedex 05, France)

Jean Benkhelil, Structural Geologist (Laboratoire de Sédimentologie et Géochimie Marines, Université de Perpignan, 52 Avenue de Villeneuve, 66860 Perpignan Cedex, France; E-mail: benkhelil@univ_perp.fr)

Emmanuel K. Brantuoh, Science Observer (Geological Survey Department, P.O. Box M80, Accra, Ghana)

Rosemary Anne Edwards, Geophysicist (Institute of Oceanographic Sciences, Deacon Laboratory, Brook Road, Wormley, Godalming, Surrey GU8 5UB, United Kingdom; E-mail: roed@uk.ac.nwo.ua)

E. (Lee) Ewert, LDEO Logging Scientist (Borehole Research, Department of Geology, University of Leicester, University Road, Leicester LE1 7RH, United Kingdom; E-mail: lee2@le.ac.uk)

Carlos Gonçalves, LDEO Logging Technician (Borehole Research, Department of Geology, University of Leicester, University Road, Leicester LE1 7RH, United Kingdom)

Ken-ichiro Hisada, Sedimentologist (Institute of Geoscience, University of Tsukuba, Tsukuba, Ibaraki, Japan 305; E-mail: hisadak@arsia.geo.tsukuba.ac.jp)

Mary Anne Holmes, Sedimentologist (Department of Geology, 214 Bessey Hall, University of Nebraska-Lincoln, Lincoln, Nebraska 68588-0340, U.S.A.; E-mail: mholmes@unlinfo.unl.edu)

Aleksandra G. Janik, Physical Properties Specialist (Rosenstiel School of Marine and Atmospheric Science, University of Miami, 4600 Rickenbacker Causeway, Miami, Florida 33149, U.S.A.; E-mail: alek@kai.rsmas.miami.edu)
Kyger C. Lohmann, Sedimentologist (Department of Geological Sciences, University of Michigan, Ann Arbor, Michigan 48109-1063, U.S.A.; E-mail: kacey@umich.edu)
Sumito Morita, Physical Properties Specialist (Ocean Research Institute, University of Tokyo, 1-15-1, Minami-dai, Nakano-ku, Tokyo 164, Japan; E-mail: moritas@ori.u-tokyo.ac.jp)
Carlos A. Mortera-Gutierrez, Paleomagnetist (Department of Geology and Geophysics, Texas A&M University, College Station, Texas 77843, U.S.A.; E-mail: mortera@tamu.edu)
Richard D. Norris, Paleontologist (foraminifers) (Woods Hole Oceanographic Institution, Woods Hole, Massachusetts 02543, U.S.A.; E-mail: dick@cod.whoi.edu)
Francisca E. Oboh, Sedimentologist (Department of Geology and Geophysics, 125 McNutt Hall, University of Missouri-Rolla, Rolla, Missouri 65401-0249, U.S.A.; E-mail: foboh@umr.edu)
Elizabeth A. Pickett, Structural Geologist (Department of Geology and Geophysics, Grant Institute, University of Edinburgh, West Mains Road, Edinburgh EH9 3JW, United Kingdom; E-mail: epickett@glg.ed.ac.uk)
Thomas Pletsch, Sedimentologist (Institut und Museum für Geologie/Paläontologie der Universität Tübingen, Sigwartstrasse 10, D-72076 Tübingen, Federal Republic of Germany: As of March 1995 - Institut und Museum für Geologie/Paläontologie der Universität Kiel, Olshausenstrasse 40-60, D-24118 Kiel, Federal Republic of Germany)
Greg Ravizza, Inorganic Geochemist (Woods Hole Oceanographic Institution, Woods Hole, Massachusetts 02543, U.S.A.; E-mail: gravizza@whoi.edu)
Samir Shafik, Paleontologist (nannofossils) (Australian Geological Survey Organisation (AGSO), Marine, Petroleum and Sedimentary Resources, GPO Box 378, Canberra City, ACT 2601, Australia; E-mail: s_shafik@bmr.gov.au)
Im Chul Shin, Paleontologist (nannofossils) (Department of Geology, 214 Bessey Hall, University of Nebraska-Lincoln, Lincoln, Nebraska 68588-0340, U.S.A.; E-mail: ishin@unl.edu)
Kari O. Strand, Sedimentologist (Department of Geosciences and Astronomy, University of Oulu, Linnanmaa, FIN-90570 Oulu, Finland; E-mail: geol-ks@finou)
Thomas Wagner, Organic Geochemist (University of Bremen, Fachbereich 5, Klagenfurter Strasse, 28359 Bremen, Federal Republic of Germany)
David K. Watkins, Paleontologist (nannofossils) (Department of Geology, 214 Bessey Hall, University of Nebraska-Lincoln, Lincoln, Nebraska 68588-0340, U.S.A.; E-mail: dwatkins@unlinfo.unl.edu)

ABSTRACT

Leg 159 drilled a series of four sites (Sites 959-962) within continental crust adjacent to the continent-ocean transition along the transform passive margin of Côte d'Ivoire-Ghana (CIG). This leg represents the first application of deep-sea drilling to the tectonics of transform margin development. A series of tectonized Albian sediments documents an early phase of intra-continental transform motion. The deep-water lacustrine sequence passes into a progressively more marine sequence as break-up continued, probably as part of a pull-apart basin system. The co-existence of compressional and extensional features, as well as rarer strike-slip faults, shows the intense deformation that affected a broad zone of the continental margin at that time. Subsequent inversion of the pull-apart basin into the Marginal Ridge occurred during the Cenomanian-Turonian. The period of maximum uplift of the ridge is shown by the development of shallow-water reefal carbonates and associated high-energy, coarse, clastic sediments of Turonian-Santonian age. Tectonic models of transform margins indicate that, following continental break-up, an active ocean-continent transform phase is ended by the migration of an active oceanic spreading center along the margin. Transfer of heat from the spreading ridge is predicted to cause major uplift and may correspond to this phase of shallow-water sedimentation. Subsequent cooling of the continental lithosphere would produce subsidence. Post-Santonian sedimentation at Site 959, situated on the flanks of the Deep Ivorian Basin, was marked by a deeper water, organic-rich, black shale facies that continued until the late Paleocene. In contrast, Sites 960, 961, and 962, which are located closer to the crest of the CIG Marginal Ridge, show hiatus and condensed claystone facies with glauconitic hardgrounds at this time. This ridge may have acted as a sill to the Deep Ivorian Basin where free circulation with the open Atlantic was restricted. A major unconformity seen at all four sites in the upper Paleocene may mark the end of rapid thermal subsidence of the margin, but may also reflect changes in current activity at that time. Much of the Eocene and Oligocene is represented by pelagic siliceous sedimentation, with slumping off the uplifted ridge crest seen at Site 959. Neogene sedimentation is dominated by a hemipelagic clayey nannofossil sedimentation, except at Site 962, which accumulated clay alone due to its position below the carbonate compensation depth (CCD). Study of the Neogene sediments at Sites 959 and 960 is expected to yield a rare, high-resolution (1,000-10,000 yr) record of the intermediate-water history in the Eastern Equatorial Atlantic, with implications for paleoceanographic changes during glacial/interglacial cycles.

INTRODUCTION

The concept of a transform (or sheared/translational) continental margin as a specific type of continent/ocean boundary progressively developed since the 1970's. Geophysical results from several transform margins clearly demonstrate that these continental borderlands are drastically different from divergent margins in terms of crustal structure, deformation, subsidence, and sedimentation history.

During the past 20 years, several marine geophysical cruises (mainly collecting gravimetry data, as well as refraction, and reflection seismic profiles) have been devoted to a few transform margins (e.g., Falklands and Exmouth plateaux). As a result, three main morphostructural features can be recognized as common to most transform margins; these include a) lateral structural continuity between a major oceanic fracture zone and a continental transform margin (e.g., the Romanche Fracture Zone and Côte d'Ivoire-Ghana Margin; Fig. 1), b) very steep and narrow continental slope (20-30 km) between a continental shelf and an adjacent oceanic abyssal plain, indicating a very sharp crustal transition between thick or partially thinned continental crust and oceanic lithosphere (Fig. 2), and c) morphologically well expressed marginal ridge bounding the transform margin, along an adjacent extensional basin (Côte d'Ivoire Basin) (Fig. 3).

Formation of a transform margin involves three major stages: an intra-continental active transform phase, a continent-ocean active transform phase, and an inactive continent-ocean transform phase. Such an evolution requires a series of different crustal/lithospheric contacts between the two plates on either side of the transform boundary. Changes in the nature of the lithosphere on either side of the transform would have led to strong thermal and pressure contrasts, which may have been recorded in the sedimentary cover of the margin at various stages in its evolution (Sage, 1994; Todd and Keen, 1989).

The objectives of Leg 159 were to

(1) determine the tectonic and sedimentary processes involved in the creation of the different main morphostructural features generated at the CIG Transform Margin, with special attention to the formation of the Marginal Ridge. A determination of the lithology and structural history of the

acoustic basement underlying the minor en-échelon ridges generated along the transform boundary was also a key objective.

(2) document the type of deformation and the deformation history of the CIG Transform Margin during its successive stages of evolution;

(3) constrain the timing, rate, and degree of vertical motion (subsidence and uplift) occurring on the CIG Transform Margin;

(4) investigate the thermal evolution of a transform margin, and compare this with the progressive westward migration of an actively spreading oceanic ridge along the southern side of the transform boundary. The thermally-driven processes to be addressed included diagenesis within the transform margin, as well as heating, hydrothermalism, and possibly magmatism occurring along the margin in response to the vicinity of the spreading center;

(5) collect data on the history the Cretaceous and Cenozoic oceanic gateways across the Equatorial Atlantic and on the sedimentation of specific facies during the opening phase. Periods of oceanic anoxia were a specific target for investigation (e.g., Jenkyns, 1980; Bralower and Thierstein, 1984), with the intention of applying new chronometric techniques, such as the Rhenium/Osmium (Re/Os) evolution of the Cretaceous seawater, in the reconstruction of the paleoenvironment (e.g., Ravizza and Turekian, 1992); and

(6) document Plio-Pleistocene changes in the character and origin of intermediate waters flowing through the Eastern Equatorial Atlantic (c.f., Oppo et al., 1994).

Regional Geology of the Côte d'Ivoire-Ghana Transform Margin

The CIG margin results from major transform motion between plate boundaries. This motion is still active today along the Romanche Fracture Zone, which offsets the Mid-Atlantic Ridge by 945 km (Fig. 1A; Fail et al., 1970). The area of particular recent investigation along this margin is the CIG Marginal Ridge which corresponds to a transition between a laterally thinned continental crust and an adjacent oceanic crust (Fig. 1B). The setting of the present-day Marginal Ridge includes a fossil ridge that connects laterally with the extinct Romanche Fracture Zone.

The seismic stratigraphy and tectonics of the area drilled during Leg 159 are primarily based on investigations by the 1983 *Equamarge I* cruise (Blarez, 1986; Blarez et al., 1987; Mascle and Blarez, 1987; Mascle et al., 1988), the 1990 *Equasis* cruise, the *Equaref* cruise, and *C. Darwin* cruise 55 (1990 and 1991, respectively), the 1988 *Equamarge II* cruise (Mascle, Auroux, et al., 1989; Basile et al., 1989; Popoff et al., 1989; Pontoise et al., 1990; Basile, 1990; Basile et al., 1992; Basile et al., 1993), the 1992 *Equanaute* cruise (Mascle et al., 1993 and 1994), and a few results from the Brazilian conjugate margin explored by PETROBRAS (Ponte and Asmus, 1978; Zalan et al., 1985; Costa et al., 1990).

Seismic Stratigraphy

The seismic stratigraphy is defined on the basis of angular relationships between several sedimentary units, especially along the northern slope of the CIG Marginal Ridge. Six main seismic units, A to F, are recognized (Fig. 4; Basile et al., 1993).

The relationships between basal Unit A and the underlying acoustic basement are unclear. This unit is deformed in both the extensional Deep Ivorian Basin and the transform Marginal Ridge. It has been divided into Subunits A0, A1, and A2, based on the presence of sequence boundaries defined on the seismic lines. A0 seems to be ante-rift in the whole area. A1 is syn-rift in the extensional Deep Ivorian Basin. A2 is post-rift in the Deep Ivorian Basin, but appears deformed within the transform margin domain.

Unit B corresponds to post-rift sediments, and is not deformed within the transform margin. It unconformably overlies both the A sequence of the extensional Deep Ivorian Basin and the A2 (syn-transform) sequence of the transform margin.

Units C to F lie conformably on the previous units, within and along the eastern side of the transform margin. However, they lie unconformably on the B and A2 sequences that constitute most of the northern Marginal Ridge slope. All units lie almost horizontally in the Deep Ivorian Basin, but may progressively pinch out against the Marginal Ridge, possibly due to coeval ridge uplift.

Sedimentary units C and D have been deposited both by aggradation within the Deep Ivorian Basin (i.e., distal detrital sedimentation from the African coast) and by progradation originating from the marginal ridge summit (i.e., proximal detrital sedimentation). Such mechanisms imply that the ridge top was near sea level at the time of their deposition, which was unknown prior to drilling. The upper part of the C sequence onlaps the ridge top, whereas the lower D sequence is restricted to the deepest part of the Ivorian Basin. Such progressive restriction of the sedimentation area also characterizes the E and F sequences.

RESULTS

Site 959

Site 959 is located in 2100 m water depth on a small plateau on the southern shoulder of the Deep Ivorian Basin (DIB). This plateau extends just north of the top of the CIG Marginal Ridge (CIGMR) (Fig. 2). Both features, the CIGMR and DIB, were generated as a consequence of Early Cretaceous rifting of the northern South Atlantic. Drilling at Site 959 penetrated seismic stratigraphic units F-B, and was designed to document the sedimentary and structural evolution of the CIG Marginal Ridge since early in the process of continental break-up. The sedimentary depositional environments and the state of tectonically induced deformation were key factors addressed by the drilling. In addition, triple recovery of the upper, less lithified sediments, was intended to provide a high-resolution paleoceanographic history of the Neogene of the central Atlantic intermediate waters, and a record of climatic change, such as desertification onshore Africa.

Four lithologic units were recognized (Fig. 5).

> Lithologic Unit I (Holocene to early Miocene; 0-208.0 mbsf) is composed of a mixture of nannofossil ooze and foraminiferal ooze, which alternates from laminated to bioturbated intervals. Subunit IA (0-23.3 mbsf), which is composed of nannofossil ooze, foraminiferal nannofossil ooze, and nannofossil ooze with clay, is dated as Pleistocene to late Pliocene. The subunit shows an increase in the content of pyrite and organic matter relative to underlying Subunit IB (23.3-208.0 mbsf), which is dated as late Pliocene to early Miocene.

> Lithologic Unit II (early Miocene to late Paleocene; 208.0-812.3 mbsf) is composed of 599.3 m of alternating siliceous and calcareous sediment, divided into three subunits. Subunit IIA (early Miocene to early Oligocene) is composed of interbedded nannofossil chalk, diatomite, and clay. A black, middle early Oligocene chert layer at 430-440 mbsf is designated Subunit IIB. Subunit IIC (early Oligocene to late Paleocene) is composed of micrite chalk and porcellanite.

Lithologic Unit III (late Paleocene to Late Cretaceous (early Coniacian); 812.3-1043.3 mbsf) is composed of 231.0 m of black claystone. Black claystone with nannofossils occurs at both the top and base of the unit. The Cretaceous/Tertiary boundary could not be identified by using microfossils, and was not marked by any notable change in the sedimentary facies. Palynomorphs were present, but were poorly preserved.

Lithologic Unit IV (Cretaceous (early Coniacian to late Albian and older); 1043.3-1158.9 mbsf) is composed of 115.6 m of sandstone, silty claystone, and limestone. Subunit IVA (1043.3-1062.7 mbsf; Cretaceous (early Coniacian to early Turonian) consists of calcarenites (sandstones and silty sandstones) with a minor quartz component. Subunit IVB (1062.7-1081.7 mbsf; early Turonian and older) consists entirely of limestones and dolomitic limestones, mostly composed of algal and molluscan shell debris. Subunit IVC (1081.7-1158.9 mbsf; late Albian and older) is composed of quartz sandstone and silty claystone.

Site 959 recovered Pleistocene to Albian and older deposits (Fig. 5). A nearly complete Neogene section with diverse calcareous microfossils is present in the upper 300 m (seafloor to Section 159-959A-32X-CC). Oligocene rocks were recovered between Sections 159-959A-33X-CC and 159-959A-43X-CC (303-428 mbsf). Middle Eocene to upper Paleocene siliceous rocks are found between Sections 159-959D-14R-CC and 159-959D-43R-CC. Between Sections 159-959D-45R-CC and 159-959D-65R-CC, only agglutinated foraminifers and pollens were found, probably of Late Cretaceous age. It is likely that an unconformity spans most of the Paleocene. Sparse nannofloras in Sections 159-959D-65R-CC to 159-959D-74R-CC indicate Santonian-Albian age. Rocks between Sections 159-959D-76R-CC and 159-959D-78R-CC are barren of siliceous and calcareous microfossils.

Most of the sediments cored in Holes 959A, 959B, and 959C are shallow dipping. At 0-47 mbsf, dips are high due to drilling disturbance. A slight increase in dip value with depth (from 2°-4° at 48-70 mbsf to 4°-15° by 400 mbsf) was observed in Hole 959A. In Hole 959D, bedding dips are relatively shallow from 420-600 mbsf but increase to 20°-30° between 960 and 1000 mbsf, before decreasing to 6°-15° between 1035 and 1044 mbsf. This change corresponds to the top of lithologic Unit IV. An abrupt increase in bedding dip (51°-83°) was recorded over the interval 1112-1140 mbsf. Geographically oriented bedding dip directions from Holes 959A and 959B indicate trends toward the north-northwest and northwest, respectively. Microfaults appear at a depth of 92 mbsf in Hole 959A and occur within most of the sequence below this level. Anastomosing normal faults, with seams of fine-grained material along fault planes and minor associated reverse faults, are a distinctive structural feature of the diatomites of lithologic Unit II. These faults are post-dated by sharply defined planar normal faults. Reorientation of the cores in Holes 959A and 959B shows a series of northeast-dipping normal faults and a conjugate set dipping northwest and southeast, respectively. Several types of vein geometry and infills were observed in Hole 959D, including barite, calcite, quartz, dolomite, and kaolinite. Two or three generations of vein growth are observed. Veins occur as tension gashes, irregular veinlets, septarian-type networks, and along faults. Many are slickensided and display evidence of shearing.

Whole-core magnetic susceptibility measurements show a low susceptibility from the seafloor to about 50 mbsf in Holes 959A, 959B, and 959C, and a gradual increase from 50 to 162 mbsf. There is a low susceptibility from about 162 mbsf to the bottom of each hole, which corresponds to an increase in clay content. Susceptibility measurements from Hole 959D show a low susceptibility from 417.8 to 1100 mbsf, and a slight rise beneath this depth in the sandstones of lithologic Unit IV. Remanence intensity is generally low (0.1-1.0 mA/m) at 0-50 mbsf. Between 50 and 162 mbsf, remanence intensity reaches 10-50 mA/m, where a drilling-induced effect dominates. Stepwise demagnetization to 25 mT indicates the presence of additional high coercivity components, but these could not be resolved shipboard. Below 162 mbsf, NRM intensity is generally low and <1 mA/m. Cores 159-959A-1H to 159-959A-4H yielded reversals in declination from which a preliminary magnetostratigraphic interpretation could be made to the base of the Matuyama reverse polarity chron, and more tentatively to the base of the Gauss normal polarity chron. This magnetostratigraphy indicates a sedimentation rate of about 7 m/m.y. since 3.5 Ma.

Interstitial water analyses indicate organic matter degradation at 0-200 mbsf. Methanogenesis is seen below the sulfate-reducing zone. Profiles of Ca, Mg, Mn, and alkalinity indicate carbonate precipitation within the zone of sulfate reduction. Carbonate dissolution and recrystallization are suggested by Sr, Ca, and alkalinity trends below 150 mbsf. Dissolved silica concentrations are high where sediments rich in biogenic silica are dissolving, and exhibit minima in portions of the section with negligible silica content. Uptake of potassium by clay minerals is likely to be responsible for a systematic decrease in pore-fluid potassium concentrations with increasing depth in the sediment.

Organic carbon contents range from 0.1 to 5.45 wt% and carbonate carbon ranges from 0 to 83 wt%. Fluctuations in these values correlate with lithology, although within lithological units, highly variable organic and carbonate carbon patterns demonstrate changes in paleoenvironmental conditions and/or different stages of diagenetic overprint. Continuous input from terrestrial sources during the Pliocene-Pleistocene is indicated by generally intermediate to low carbonate contents (25-55 wt%) and elevated organic carbon vs. total nitrogen ratios (10-20). Carbonate and organic carbon profiles in Miocene and Oligocene interbeds of TOC-rich diatomites and porcellanites indicate carbonate dissolution due to degradation of labile organic matter. Thermally immature organic matter (T_{max} 400°-420°C) is characteristic for diatomites and porcellanites. The highest TOC contents were measured in Upper Cretaceous black claystones. A dominant African terrestrial source of the organic matter is shown by high C/N ratios and intermediate hydrogen indices (150-250 mgHC/gTOC). Very high contents of thermally overmature (T_{max} 465°-485°C) organic matter were found at the bottom of Hole 959D. C_1/C_{2+} ratios indicate that thermogenic processes had occurred in the geologic past, as anticipated before the cruise.

The physical properties data at Site 959 are heterogeneous, reflecting variations in consolidation, age, and lithology. The most important discontinuities occur at 150 mbsf, 456 mbsf, and 750 mbsf. The discontinuity at 150 mbsf does not correspond to a change in lithology. At 456 mbsf, the change coincides with a change from nannofossil chalk and clay to chert. The discontinuity at 750 mbsf occurs in an interval with no change in lithology, but a noted increase in clay and decrease in opal. The scatter in values of physical properties is generally very narrow, suggesting that few small-scale heterogeneities exist in sediments at Site 959 (especially in lithologic Units I to III).

Downhole measurements were successfully conducted in the lower part of Hole 959D (395-1077 mbsf). The logs are of generally excellent quality throughout the logged sequence despite limited deterioration due to borehole washout near the top (405-425 mbsf) and bottom (1025-1045 mbsf) of the logged interval. Initial comparison between log and core data shows good correlation for natural gamma ray and velocity measurements. Preliminary interpretation of the formation microscanner (FMS) data shows bedding planes dipping consistently toward north-northwest with increasing dips downhole (from 20° at 550 mbsf to >40° at 850 mbsf).

<u>Site 960</u>

Site 960 is located 3 miles south of Site 959 in 2061 m water depth, on a small plateau that occupies the summit of the CIGMR at 2000 m (Fig. 2). Originally planned as an alternate to Site 959, the sedimentary cover above seismic unit A is much reduced (Fig. 6), and Site 960 was drilled to sample this lowermost unit.

Five lithologic units were identified from Holes 960A and 960C (Fig. 7).

Lithologic Unit I (Pleistocene to early Miocene; 0-111.2 mbsf) is composed of 111.2 m of Pleistocene nannofossil/foraminifer ooze (Subunit IA) and nannofossil/foraminifer chalk (Subunit IB). The first appearance (at 100.1 mbsf in Hole 960A and 111.2 mbsf in Hole 960C) of siliceous microfauna and flora marks the upper boundary of lithologic Unit II.

Lithologic Unit II (early Miocene and early to middle Eocene; 111.2-179.0 mbsf) is characterized by radiolarian/nannofossil chalk, claystone, and porcellanite of early Miocene and middle Eocene age (Subunit IIA), and chert of early to middle Eocene age (Subunit IIB). A large stratigraphic break is inferred between these two subunits (Fig. 7), although poor recovery meant that the nature of any unconformity/condensed sequence is unknown. The lithologic Unit II/III boundary (164.8 mbsf in Hole 960A and 179.0 mbsf in Hole 960C) is marked by the last occurrence of chert and the presence of a palygorskite-rich claystone interval containing barite concretions and nodules.

Lithologic Unit III (early Eocene; 179.0-198.8 mbsf) is a 20.5 m (Hole 960A) to 18.7 m (Hole 960C) thick unit, distinguished by its bluish-green color and abundant authigenic barite.

Lithologic Unit IV (Masstrichtian to Turonian; 198.8-329.0 mbsf) is subdivided into lithologic Subunit IVA, a condensed (<10 m) interval with fish debris, hardgrounds, glauconitic claystones, and micritic chalks (Maastrichtian-Coniacian) and lithologic Subunit IVB (Turonian and older), a <144.9 m thick unit composed of quartz sand and skeletal packstones and grainstones. The top is identified as the first occurrence of bioclastic and intraclastic limestones, which contain variable amounts of quartz sand. The lower boundary is placed where bioclastic limestones of lithologic Subunit IVB overlie carbonate-cemented quartz sandstones of lithologic Unit V.

Lithologic Unit V (Turonian and Albian and older; 329.0-451.2 mbsf) is 122.2 m thick. Carbonate-cemented sandstones and siltstones are found in lithologic Subunit VA, changing to silty sandstones, siltstones, and clayey siltstones of possible lacustrine origin in lithologic Subunit VB.

Pleistocene to early Eocene nannofossils were identified in the first 20 cores of Hole 960A. This sequence is interrupted by two barren intervals, and probably contains at least two major hiatuses.

Middle Miocene Zone CN5 is missing. Nannofossils representing the time interval from Zone CP14 (middle Eocene) through to the top of Zone CP19 (late Oligocene) are missing. A barren interval is identified at about the Neogene/Paleogene boundary. The lower/middle Eocene section contains a barren interval near its base. Nannofossil assemblages range from Turonian to Pleistocene in Core 159-960C-1H through Section 159-960C-26X-CC. Within this sequence, at least three pronounced hiatuses could be detected. One of these hiatuses is between early Miocene and middle Eocene assemblages. The youngest hiatus is within Core 159-960C-10H, separating sediments of Zone CN7 (late Miocene) from those of Zone CN4 (early middle Miocene). The oldest hiatus is within Core 159-960C-23X, between assemblages assignable to the early Eocene Zone CP9 and others of Coniacian to Santonian age.

Bedding dips at 0-150 mbsf in Hole 960C display a wide range of values, largely due to slumping. The unconformity at the lithologic Unit IV/V boundary is characterized by fissuring, veining, and brecciation. The bedding dip data collected from Unit V show a wide spectrum (5°-60˚), with the steeper dips measured directly below the unconformity, where the majority of faulting and veining observed also occurs. Calcite and kaolinite veins are abundant, with quartz veins appearing at the bottom of Hole 960A (450 mbsf). Complex microfaulting, with associated asymmetric microfolds, displays both normal and reverse senses of motion, possible evidence for strike-slip flower structures. Oblique slickensides/mineral lineations in kaolinite-filled faults also clearly indicate strike-slip.

Magnetic measurements indicate three distinctive transitions in magnetic properties, which can be correlated between Holes 960A and 960C, and Site 959. A sharp increase in NRM intensity and in bulk susceptibility occurs at the upper/lower Pliocene boundary (32 mbsf in Hole 960C, 20 mbsf in Hole 960A). A drop in intensity of magnetization and in susceptibility was encountered at 92 mbsf in Hole 960C and at 74 mbsf in Hole 960A, corresponding to a major hiatus between the upper Miocene and lower middle Miocene. An unconformity was found at 329 mbsf in Hole 960A, where both the intensity of magnetization and the bulk susceptibility increase significantly. The remanence direction, where measured, is dominated by a drilling-induced component, the character of which alternates in successive cores. This alternation corresponds to the sequential use of two separate APC inner core barrels, which may be inducing the magnetization. Demagnetization to 25 mT does not isolate a high coercivity component, but does define a great-circle trajectory, suggesting that a high coercivity component is present, which may be determined by cleaning in stronger fields.

At 0-100 mbsf, microbial degradation of organic matter drives the sequential reduction of manganese, iron, and sulfate in the sediment, with these reactions occurring at less than 10 mbsf, at 10 mbsf, and at approximately 30 mbsf, respectively. Below 100 mbsf, the small number of samples precludes making a detailed interpretation of pore-fluid chemistry, but alkalinity and ammonium data indicate that the deeper sediments at Site 960 are less influenced by organic matter degradation. Profiles of dissolved Ca, Mg, and Sr reflect major differences between pore-fluid chemistry at Sites 959 and 960. At Site 960, no minimum in dissolved Ca occurs. An increase in Mg and an increase in Sr downhole suggest carbonate recrystallization but not carbonate precipitation.

Organic carbon contents range from 0 to 6.44 wt%, and carbonate contents from 0 to 98 wt%. These concentrations are controlled by paleoenvironmental conditions and/or degree of diagenesis. Intermediate carbonate contents (35-55 wt%), elevated C/N ratios (10-14), and low hydrogen indices (<100 mgHC/gTOC) are seen in the upper Pliocene to Pleistocene. An increase in organic carbon (5.6 wt%) correlates to a drop in carbonate (0 wt%) at the Miocene/Pliocene boundary. A very high C/N ratio and a low hydrogen index suggest deposition of terrestrial, oxidized organic matter. Early Eocene to early Miocene chalks and claystones indicate a mixed marine/terrestrial source for the organic matter, while the underlying limestone unit has no organic carbon. Highly variable organic carbon records with peak contents above 2 wt% and minimum carbonate contents are characteristic of lithologic Unit V. Low hydrogen indices and C/N ratios indicate a terrestrial source. T_{max} values suggest a mixture of immature (below 365˚C) and overmature (above 450˚C) organic matter.

Natural gamma measurements from core are low at 0-100 mbsf, then rise due to increasing glauconite content. Natural gamma is also high in the palygorskite clay of lithologic Unit III. P-wave velocity is 1.5 km/s in lithologic Units I and II, increasing to 4.0-6.0 km/s in the limestones of lithologic Unit IV, but falling again to 2.5-4.5 km/s in the claystones and sandstones of lithologic Unit V. P-wave velocity also peaks at the late to mid-Miocene boundary. No lithologic change is noted, but biostratigraphic evidence indicates a disconformity.

The quad combo tool string covered the interval from 361.3 to 73.3 mbsf in Hole 960A. Only one-third of the logged open hole interval was of a diameter less than 16 in. (as shown by the caliper curve), and these conditions seriously affected the quality of the sonic, density, and porosity data collected by the tool string. Resistivity and gamma ray data were affected to a much lesser degree. The FMS and GLT tool strings were not run in Hole 960A. In Hole 960C, a natural gamma, resistivity, and sonic tool string was run between 121.2-92.4 mbsf and 374.6-159.7 mbsf. Again, the caliper curve indicated washed-out conditions for over half of the logged interval, resulting in poor quality sonic data. The FMS was run but was unable to get past a bridge and so covered the interval 354.5-173.7 mbsf. Data quality was understandably poor, but may improve when processed onshore.

Site 961

Site 961 lies in 3303 m water depth on the last significant morphologic expression of the CIGMR just before its burial, toward the west, beneath the thick sedimentary cover of the Deep Ivorian Basin (Fig. 2). In the area, a multichannel seismic (MCS) line recorded along strike of the CIGMR shows that the progressively deepening pre- and syn-rift basement consists of a series of rotated structural blocks and bordering half grabens (Fig. 8), each about 5 km across. Detailed structural mapping clearly indicates that these extensional structures are bounded by north-south- trending fault zones and are rather similar, in trends and in size, to second order extensional blocks detected within the northern adjacent rifted Deep Ivorian Basin.

In Hole 961A, 308.7 m of stratigraphic section was cored. In Hole 961B, the top 216.3 mbsf, and the intervals 239.0-259.9 mbsf and 264.9-267.5 mbsf, were drilled without coring.

Three lithologic units were identified at Site 961 (Fig. 9).

Lithologic Unit I (Pleistocene to early Miocene; 0-129.5 mbsf) is composed of nannofossil ooze with foraminifers, which grades downhole into clayey nannofossil chalk and claystone. It is divided into two subunits, Subunit IA (Pleistocene to late Pliocene; 0-16 mbsf) having a darker color because of higher pyrite and organic matter contents and Subunit IB (early Pliocene to early Miocene; 16-129.5 mbsf). Lithologic Unit I at this site can be correlated with lithologic Unit I at Sites 959 and 960. The top boundary of lithologic Unit II (129.5-188.5 mbsf) is marked by the first significant appearance of siliceous microfossils in the sediments.

Lithologic Unit II (early Miocene, early Eocene, late Paleocene and older; 129.5-188.5 mbsf) is also divided two subunits. Subunit IIA (129.5-148.1 mbsf) is composed of early Miocene nannofossil chalk with radiolarians and glauconite, and claystone with glauconite. Subunit IIB (148.1-188.5 mbsf) consists of chert interbedded with clayey porcellanite with micrite and zeolite, palygorskite/zeolite claystone, and glauconite-rich porcellanite (early Eocene to late Paleocene and older). Lithologic Unit II correlates with Unit II at Site 959 and with Units II and III at Site 960.

Lithologic Unit III (unknown age in upper part; below 303 mbsf, Maastrichtian to Bajocian; 188.5-374.6 mbsf) consists of dark gray to black silty sandstone, sandy siltstone, clayey siltstone, and silty claystone, with local pyrite and siderite. This unit is correlated with Subunit VA at Site 960. Age is constrained poorly, being some time during the Maastrichtian to Bajocian.

Pleistocene sediments were recovered in Hole 961A at 3.4 mbsf. A Pliocene section extends from 13.1 mbsf to the Miocene/Pliocene boundary at 32.3 mbsf. Below a middle to upper Miocene interval that extends to 148.1 mbsf, an unconformity has removed most or all of the Oligocene and the middle to upper Eocene. There may also be an unconformity or condensed interval in the upper middle Miocene at 81-100 mbsf. The lower Eocene is present from 157.8 to 167.4 mbsf, and the upper Paleocene from 177.0 to 186.7 mbsf. Below this, the section is barren of calcareous and siliceous microfossils. Hole 961B is barren of planktonic foraminifers. Only one species of calcareous nannofossil has been identified at 313.2 and 322.4 mbsf. This taxon ranges from the Bajocian through the Cretaceous. Calcareous microfossil preservation generally deteriorates downsection, and planktonic foraminifers are absent below the lower Miocene.

In Hole 961A, very little bedding data were recorded due to poor recovery and drilling disturbance. A few normal faults were observed in Hole 961A. Variable dips in Hole 961B can be attributed, at least partly, to synsedimentary disturbances (convolute bedding, slump fold) and faults. We observed sets of conjugated normal faults (Section 159-961B-18R-1) and steeply dipping shears (Core 159-961B-13R). In Core 159-961B-13R, the finely laminated bedding is affected by microfolds closely associated with small-scale shear planes. Calcite veining infilling fractures and breccia is found in the upper few cores of Hole 961B. Soft sedimentary deformations were observed in both Holes 961A and 961B and include a water-escape structure and a sand pipe, slump folds, and wavy to convolute bedding.

Changes in magnetic susceptibility mirror lithological changes, with susceptibilities of 10×10^{-5} SI units encountered in Subunit IA, and higher susceptibilities, between 10 and 50×10^{-5} SI units, in Subunit IB. Unit II has low susceptibilities, $< 15\times 10^{-5}$ SI units, and Unit III has high susceptibilities, typically between 10 and 40×10^{-5} SI units. RCB coring caused a high degree of drilling disturbance, so measurements of the direction of magnetization have no geological significance. The variation of the intensity of NRM downhole shows a similar pattern as at previous sites. NRM intensity increases from <10 mA/m in Core 159-961A-1R to up to 50 mA/m in Core 159-961A-3R. This change occurs at the transition between lithologic Subunits IA and IB, within planktonic foraminifer Biozone M9. NRM intensities in Unit II are low (<1 mA/m), except for Cores 159-961-20R and 159-961-21R, which also show a marked reduction in palygorskite content. These cores have NRM values up to 10 mA/m. NRM values remain at this level throughout Unit III.

Eight interstitial water samples were taken during coring operations at Site 961. In spite of the discontinuous sample suite, the data demonstrate a set of diagenetic reactions analogous to those documented at Sites 959 and 960. Sulfate, potassium, and magnesium concentrations decrease with increasing depth, while the concentrations of calcium and ammonium increase with increasing depth in the sediment. Appreciable pore-fluid sulfate concentrations, approximately 6 mM, persist below the depth in the sediment where methane concentrations rise above background levels. These results are suggestive of contamination of the deep (>250 mbsf) interstitial water samples with seawater. However, none of the pore-water profiles show the large degree of scatter which is expected to be associated with large and variable amounts of seawater contamination.

Generally lower carbonate and organic carbon contents in Holes 961A and 961B compared to Sites 959 and 960 are related to the more pelagic depositional conditions. Pliocene to Pleistocene deposits display highest carbonate contents (up to 50 wt%). In the upper 70 mbsf, evidence for intense organic matter degradation was found by a continuous exponential decrease in organic carbon content with depth. Paleocene through Miocene sediments have low carbonate and organic carbon contents (below 10 wt% and below 0.2 wt%, respectively). Intermediate organic carbon contents (about 0.4 wt%), but low carbonate contents, characterize the underlying sandstone and siltstone below 220 mbsf. The few maxima in organic carbon (up to 0.7 wt%) within these lithologies were probably caused by an enhanced supply of terrigenous organic matter. A vertical offset of about 10 m is proposed for Holes 961A and 961B deposits according to the matching of both carbonate and organic carbon records. In Hole 961A, very low headspace methane concentrations were recorded. A maximum methane content of 991 ppm was observed in Core 159-961A-34R (303.5 mbsf). No ethane was recorded. In Hole 961B, slightly higher readings of methane were seen. A maximum concentration of 7310 ppm was recorded in

Core 159-961B-13R (333.6 mbsf), but no ethane was detected.

General correlation between different sets of physical properties data at Site 961 is good, but the low density of measurements does not permit more detailed studies. All physical properties data collected at Site 961 show a very distinctive change in trend at the boundary between lithologic Units II and III at 188 mbsf, attributable to significant lithological differences.

Site 962

Site 962 is located on MCS line MT01 (shot point 2190), in 4650 m water depth, on a small topographic bench which extends toward the southwest, in the same direction as the CIGMR southern slope (Fig. 2). MCS line MT01 (Fig. 10), and the crossing single channel line, reveal that this small bathymetric high is in fact the subdued topographic expression of a narrow "basement" structural high, which lies between a thick pile of undeformed sediments to the south, and a fault-bounded and rather deformed basin and wedge system to the north, comprising sedimentary reflectors (Fig. 10). A dense set of single channel seismic lines reveals a similar feature just a few kilometers to the southwest. These two acoustic basement ridges, buried by sediments, are elongated (2-3 km wide and 12-15 km long), almond-shaped, and trend southeast-northwest. They lie at the boundary between the southwesternmost extension of the CIGMR and the flat-lying sediment cover of the adjacent oceanic crust to the south (Basile et al., 1993). The minor ridges are arranged en échelon according to the structural mapping of Basile (1990), and lie at the transition between the main continental transform Marginal Ridge and the oceanic fossil Romanche Fracture Zone, which is expressed in a series of aligned, still exposed, acoustic basement highs just a few kilometers toward the west-southwest.

Drilling in four holes at Site 962 penetrated 393.5 mbsf. The recovered sediment has been divided into three lithologic units (Fig. 11).

> Lithologic Unit I (late Pleistocene to early Miocene; 0-47.0 mbsf) is composed of 47 m of hemipelagic silty clays and clays. This is subdivided into two subunits. Subunit IA (middle Pleistocene to early Pliocene; 0-26.5 mbsf) consists of silty clays with opal, micrite, plant debris, and clay with nannofossils and pyrite. Subunit IB (late Miocene to early Miocene; 26.5-47.0 mbsf) is a pelagic clay which consists of quartz silt, claystone with quartz silt, and claystone.

Lithologic Unit II (early Miocene, unknown, and late Albian; 47.5-123.5 mbsf, Hole 962D) is composed of siliceous pelagic components, radiolarians and diatoms, palygorskite, and chert and porcellanite, and has been divided into three subunits. Subunit IIA (early Miocene; 47.0-64.5 mbsf) is dominated by grayish green claystone, interbedded with claystone with diatoms, radiolarians, and glauconite. Carbonate is absent in this lithologic subunit. Subunit IIB consists of greenish to bluish gray palygorskite claystone, manganese nodules, and glauconitic silty sands. This subunit occurs at 64.5-69.9 mbsf in Hole 962B, and at 73.0-83.1 mbsf in Hole 962C. Subunit IIC (Cenomanian to late Albian) is composed of brown chert and porcellanite, which is chaotically intermixed within a clayey sediment. Subunit IIC has been recovered from 69.9 to 100.0 mbsf in Hole 962B, 83.1 to 102.4 mbsf in Hole 962C, and 75.1 to 123.5 mbsf in Hole 962D.

Lithologic Unit III (late Albian; 123.5-393.5 mbsf, Hole 962D) is composed of normally graded siliciclastic sandstones, siltstones, and claystones intermixed with micritic limestones, containing planktonic foraminifers and nannofossils of late Albian age. Numerous fining-upward sequences are apparent.

The Cenozoic is greatly condensed compared to Sites 959 and 961. Preservation of calcareous microfossils is generally poor. The upper Pleistocene (0-16.8 mbsf) is relatively expanded and lies disconformably on about 5 m of upper Pliocene nannofossil claystone, which, in turn, disconformably overlies 4 m of lower Pliocene claystone. The interval between 26.5 and 36.4 mbsf is essentially barren, although a few isolated specimens of planktonic foraminifers suggest an early Pliocene to latest Miocene age. The interval between 36.4 and 45.9 mbsf is barren, but silicoflagellates and radiolarians at 50-64.0 mbsf indicate a late early Miocene age. A disconformity at 65.8 mbsf separates Cenozoic deposits from Albian-(?)Cenomanian cherts and mudstones. The presence of a distinctive palygorskite clay-bearing sequence immediately overlying this disconformity suggests, by lithologic correlation, that lower Eocene sediments may be present in Core 159-962B-8H. Upper Albian to Cenomanian radiolarians and silicified planktonic foraminifers are present at 71.3 mbsf, although the severely disturbed nature of Core 159-962B-8H makes it impossible to assess whether these microfossils are in place or were reworked during a later slumping event. This sequence is underlain by more than 300 m of deformed upper Albian (*R. appenninica* Zone; CC9) turbidites.

In Hole 962B, the few bedding measurements recorded in lithological Units I and II range from 1˚ to 18˚. In Hole 962D (lithological Unit III), there is a wide range of bedding dip values, mostly due to folding and faulting. Vertical dips, related to tectonic deformations, were recorded between 180 and 185 mbsf and between 386 and 393 mbsf. Unit III shows rare convolute bedding and slump folding throughout. Normal faulting is common. At 123 mbsf, conjugated normal faults are seen to have been formed prior to the tilting of the bedding. Reverse microfaults, both alone or associated with asymmetrical folds, are observed at various depths. Microfolding is widespread in Hole 962D, showing various morphologies from rounded (e.g., at 278 mbsf) to incipient kink folding (e.g., at 366 mbsf). Most of the folds are asymmetric, except where associated with pop-up structures (e.g., at 314 mbsf). Rare evidence of strike-slip motion includes low pitching slickensides along fault planes and flower-type structures (at 301 and 372 mbsf) where normal and reverse faults are associated. Brecciation and veining occur as infilling of extensional features (e.g., at 366 and 386 mbsf).

In Hole 962B, the magnetic susceptibility is low ($<20 \times 10^{-5}$ SI units) at 0-16 mbsf, and increases to 30×10^{-5} SI units at about 25.5 mbsf, the boundary between lithologic Subunits IA and IB. Magnetic susceptibility remains at this level to about 45 mbsf and, below this, falls to values of $<15 \times 10^{-5}$ SI units, except for an interval between about 65 and 70 mbsf, lithologic Subunit IIB, where values rise to $>30 \times 10^{-5}$ SI units. Susceptibilities throughout Hole 962D are low, generally $<15 \times 10^{-5}$ SI units. NRM intensities show a similar pattern to that of the susceptibility. A zone of high NRM intensity within the Neogene was encountered at Sites 959 and 961. The upper boundary of this zone was always at Biozone PL3/PL2 or older, and the lower boundary was at Biozone M9 or younger. If the same age relationships apply at this site, it suggests that the depth interval between 25.5 and 45 mbsf is younger than Biozone M9, and older than the Biozone PL3/PL2 boundary. Core 159-962B-5H yielded a reversal stratigraphy after cleaning isolated a stable component. This magnetostratigraphy can be correlated with Chron 3A (Messinian-late Tortonian).

Five water samples taken from 0 to 80 mbsf in Hole 962B reflect the relatively low abundances of calcium carbonate and reactive organic matter, compared to Sites 959 and 961. Gradients associated with sulfate reduction and ammonium generation are less steep than at shallower sites, indicating that organic matter degradation is less vigorous, although organic carbon contents are relatively high, up to 1.5%. Therefore, the bulk of the organic carbon in the upper portion of the sediment pile at Site 962 must be refractory and not readily degraded, in agreement with its anomalously high hydrogen values. Downcore decreases in magnesium concentrations, and increases in calcium concentrations, are significantly less pronounced than at previous sites due to low calcium carbonate contents. The downhole increase in dissolved strontium concentrations is comparable to that at Site 959, implying that dissolution/recrystallization reactions may be more intensive at Site 962. Results from Rock-Eval pyrolysis of Pleistocene sediment show a dominance of reworked, fossil organic matter. Carbonate contents are generally low, due to the site being below the CCD, except during the early Pliocene. Upper Albian porcellanites (70-100 mbsf) have high organic carbon and low carbonate contents. High C/N ratios and intermediate hydrogen indices suggest a mixed terrestrial and marine origin of the organic matter. Between 150 and 195 mbsf, peaks in organic carbon (up to 3.5 wt%) probably indicate periods of high productivity. Hydrogen indices show a low thermal maturity of marine organic matter. Decreasing hydrogen indices downcore show a stronger terrestrial influence earlier in the late Albian. The pyrolytic character does not reflect changes in lithology. Hydrocarbon gases were found in significant quantities in Hole 962D. Maximum recorded methane content was 102,214 ppm at 316 mbsf. Heavier hydrocarbons (C_2-C_6) were also present throughout. Ethane (C_2) concentrations, up to a maximum of 1401 ppm, were seen at 335 mbsf. Propane through hexane were present in trace amounts only.

Physical properties reflect variations in lithology, consolidation, and composition of sediments. Good GRAPE and NGR measurements were made in Hole 962B. The most important discontinuities in physical properties data in Hole 962B are at 47 mbsf and 70 mbsf, and they correspond to the boundaries between lithologic Units I and II and Subunits IIB and IIC. The first discontinuity at 47 mbsf is best reflected in MST, thermal conductivity, and index properties data. There is a rapid increase of bulk density and a rapid drop of porosity of sediments at 70 mbsf and an increase in NGR and GRAPE densities to higher, but more scattered, values. The boundary between lithologic Units II and III, at 123 mbsf, is reflected in discrete velocity measurements. Greater lithification below 90 mbsf is shown in index properties data as lower porosity (<30%). Bulk density values are generally higher (around 2.5 g/cm^3).

Bridging prevented the seismic stratigraphic tool string (a reduced quad combo tool string measuring only natural gamma radiation, resistivity, and sonic data) from reaching the bottom 65 m of the hole. The log covered from 328 to 162 mbsf, and a repeat log covered from 306.5 to 173 mbsf. Approximately 50% of the logged interval was of a diameter greater than 14 in., which seriously affected the quality of the sonic data collected. Resistivity and gamma ray data may also have been affected, but to a much lesser degree. The FMS was run but was unable to get past a bridge at 293 mbsf. Two passes of the FMS each covered the interval from 293 to 192 mbsf.

SUMMARY

The initial results suggest an Early Cretaceous history of restricted intra-continental sedimentation, followed by a progressive marine transgression, presumably reflecting the advancing rifting. Strong deformation observed in the oldest sediments at each of the drill sites (Fig. 12) testifies to the continuous shearing that the margin suffered during the period of intra-continental transform. At the two shallowest sites (Sites 959 and 960; Fig. 2), located in approximately 2100 m of water, a period of shallow-water shelf sedimentation during the Turonian-Santonian marks a departure from the normal subsidence pattern of a rifted passive margin, which would predict more rapid thermal subsidence shortly after continental break-up. The development of a reef near Sites 959 and 960 provides firm evidence for the uplift of the ridge at this time (Fig. 13). At Sites 961 and 962, the Turonian-Santonian, with the subsequent younger part of the Cretaceous sequence, is noted as probably one of unconformity, although the biostratigraphy does not prove this conclusively at Site 961. The tilting and uplift inferred from the sediments are believed to reflect generation of the Marginal Ridge due to transform deformation, causing flexural uplift and/or crustal thickening (Basile et al., 1993). In addition a thermal rejuvenation, and thus uplift, of the crust adjacent to the transform margin is expected due to the close proximity of an oceanic spreading center, which abutted against the margin at this time during its progressive westward migration (Mascle and Blarez, 1987). The analysis of the tectonic evolution of the Côte d'Ivoire-Ghana Marginal Ridge which this drilling allows affords a unique opportunity to test geophysical models of transform margin evolution (e.g., Todd and Keen, 1989).

The sedimentary sequences recovered also provide a rare opportunity to examine the evolution of what was an important oceanic gateway region between the Southern and Central Atlantic basins, when the Equatorial Atlantic was still a narrow seaway in this region. Most recently, the sedimentary cover to the marginal ridge, and thus Sites 959 and 960, have acted as a record of the evolution of intermediate waters in the eastern Equatorial Atlantic, as they lie at around 2100 m water depth. Through carbon and oxygen isotopic studies of the foraminifers from Sites 959-960, a high-resolution record of the intermediate waters of the equatorial oceans can be reconstructed. This will have strong implications for models of thermohaline circulation and how this evolved during and since the onset of major glaciation (e.g., Oppo et al., 1994; Raymo et al., 1989).

REFERENCES

Basile, C., 1990. Analyse structurale et modélisation analogique d'une marge transformante: l'exemple de la marge profonde de Côte d'Ivoire-Ghana. *Mém. Doc. CAESS Rennes*, 39:0-220.

Basile, C., Brun, J.P., and Mascle, J., 1992. Structure et formation de la marge transformante de Côte d'Ivoire-Ghana: apports de la sismique réflexion et de la modélisation analogique. *Bull. Soc. Géol. France*, 163:207-216.

Basile, C., Mascle, J., Auroux, C., Bouillin, J.P., Mascle, G., Gonzalves de Souza, K., and le groupe *Equamarge*, 1989. Une marge transformante type: la marge continentale de Côte d'Ivoire-Ghana: résultats préliminaires de la campagne *Equamarge II. C. R. Acad. Sci. Paris*, 308, Série II:997-1004.

Basile, C., Mascle, J., Popoff, M., Bouillin, J.P., and Mascle, G., 1993. The Côte d'Ivoire-Ghana transform margin: a marginal ridge structure deduced from seismic data. *Tectonophysics*, 222:1-19.

Blarez, E., 1986. La marge continentale de Côte d'Ivoire-Ghana: structure et évolution d'une marge continentale transformante. Ph.D. Thesis, Université Pierre et Marie Curie, 188 pp.

Blarez, E., Mascle, J., Affaton, P., Robert, C., Herbin, J.P., and Mascle, G., 1987. Géologie de la pente continentale ivoiro-ghanéenne: résultats de dragages de la campagne *Equamarge*. *Bull. Soc. Géol. France*, 5:877-885.

Bralower, T.J., and Thierstein, H.R., 1984. Low productivity and slow deep water circulation in mid-Cretaceous oceans. *Geology*, 12:614-618.

Costa, I.G., Beltrami, C.V., and Alves, L.E.M., 1990. A evoluçao tectono-sedimentar e o habitat do oleo da bacia do Ceara. *B. Geoci. PETROBRAS*, 4:65-74.

Duplessy, J.C., Shackleton, N.J., Fairbanks, R.G., Labeyrie, L.D., Oppo, D., and Kallel, N., 1988. Deepwater source variations during the last climatic cycle and their impact on the global deepwater circulation. *Paleoceanography*, 3 (3):343-360.

Fail, J.P., Montadert, L., Delteil, J.R., Valery, P., Patriat, P., and Schlich, R., 1970. Prolongation des zones de fractures de l'océan Atlantique dans le golfe de Guinée. *Earth Planet. Sci. Lett.*, 7:413-419.

Jenkyns, H.C., 1980. Cretaceous anoxic events: From continents to oceans. *J. Geol. Soc. London*, 137:171-188.

Mascle, J., Auroux, C., and the shipboard scientific team, 1989. Les marges continentales transformantes ouest-africaines (Guinée, Côte d'Ivoire-Ghana) et la zone de fracture de la

Romanche: Campagne *Equamarge II* (Février-Mars 1988). Campagnes Océanographiques Françaises. Publications IFREMER, 150 pp.

Mascle, J., and Blarez, E., 1987. Evidence for transform margin evolution from the Côte d'Ivoire - Ghana continental margin. *Nature*, 326:378-381.

Mascle, J., Blarez, E., and Marinho, M., 1988. The shallow structures of the Guinea and Côte d'Ivoire - Ghana transform margins: their bearing on the equatorial Atlantic Mesozoic evolution. *Tectonophysics*, 155:193-209.

Mascle, J., Guiraud, M., Basile, C., Benkhelil, J., Bouillin, J.P., Cousin, M., and Mascle, G., 1993. The Côte d'Ivoire-Ghana transform margin: preliminary results from the *Equanaute* cruise (June 1992). *C. R. Acad. Sci. Paris*, 316:1255-1261.

Mascle, J., and the Scientific Party, 1994. Les marges continentales transformantes ouest-africaines - Côte d'Ivoire, Ghana, Guinée., *IFREMER, Série Repères Océan*, 5:0-135.

Ponte, F.C., and Asmus, H.E., 1978. Geological framework of the Brazilian continental margin. *Geol. Rund*., 67:201-235.

Pontoise, B., Bonvalot, S., Mascle, J., and Basile, C., 1990. Structure crustale de la marge transformante de Côte d'Ivoire-Ghana déduite des observations de gravimétrie en mer. *C. R. Acad. Sci. Paris*, 310:527-534.

Popoff, M., Raillard, S., Mascle, J., Auroux, C., Basile, C., and *Equamarge* group, 1989. Analyse d'un segment de marge transformante du Ghana: résultats de la campagne Equamarge II (Mars 1988). *C. R. Acad. Sci. Paris,* 309:481-487.

Ravizza, G., and Turekian K.K., 1992. The Os isotopic composition of organic-rich marine sediments. *Earth Planet. Sci. Lett.,* 10:1-6.

Raymo, M., Ruddiman, W.F., Backman, J., Clement, B.M., and Martinson, D.G., 1989. Late Pliocene variation in Northern Hemisphere ice sheets and North Atlantic Deep Water Circulation. *Paleoceanography,* 4:413-446.

Sage, F., 1994. Structure Crustale d'une Marge Transformante et du Domaine Océanique Adjacent: exemple de la marge de Côte d'Ivoire-Ghana. Ph.D. Thesis, Université Paris VI, 339 pp.

Todd, B.J., and Keen, C.E, 1989. Temperature effects and their geological consequences at transform margins. *Can. J. Earth Sci*., 26:2591-2603.

Zalan, P.V., Nelson, E.P., Warme, J.E., and Davis, T.L., 1985. The Piaui basin: rifting and wrenching in an Equatorial Atlantic transform basin. *In* Biddle, K.T., and Christie-Blick, N. (Eds.), *Strike-slip deformation, basin formation and sedimentation*. N. Soc. Econ. Paleont. Miner., Spec. Publ., 37:143-158.

FIGURE CAPTIONS

Figure 1A. Fracture zones of the equatorial Atlantic and associated continental margins.

Figure 1B. Geodynamic sketch of the Côte d'Ivoire Ghana Margin and the different ocean/continent transitions. Shaded areas are oceanic fracture zones and marginal ridges.

Figure 2. Detailed swath bathymetric map showing the location of the Leg 159 drill sites.

Figure 3. A typical multichannel seismic line (MT02) across the Deep Ivorian Basin and the Marginal Ridge. Location of line is shown in Figure 2.

Figure 4. Enlarged section of MCS line MT02 and location of Site 959.

Figure 5. Simplified lithostratigraphy and ages of sediments cored at Site 959. G = glauconite. Py = pyrite. Ba = barite.

Figure 6. Enlarged section of MCS line MT02 and location of Site 960.

Figure 7. Simplified lithostratigraphy and ages of sediments cored at Site 960. Pa = palygorskite.

Figure 8. Enlarged section of MCS line MT05 and location of Site 961.

Figure 9. Simplified lithostratigraphy and ages of sediments cored at Site 961.

Figure 10. Enlarged section of MCS line MT01 and location of Site 962.

Figure 11. Simplified lithostratigraphy and ages of sediments cored at Site 962.

Figure 12. Summary of the structures observed at Sites 960, 961, and 962 along the strike of the Marginal Ridge. Note that the most pervasive deformation and compressional deformation are confined to the Lower Cretaceous, the lower parts of each drill site.

Figure 13. Three main stages in the evolution of the Côte d'Ivoire-Ghana Margin (view from the west-northwest). Stage A - stippled areas show syn-rift basins (divergent basins and marginal ridge). Stages B and C - shaded belt includes main transform domain.

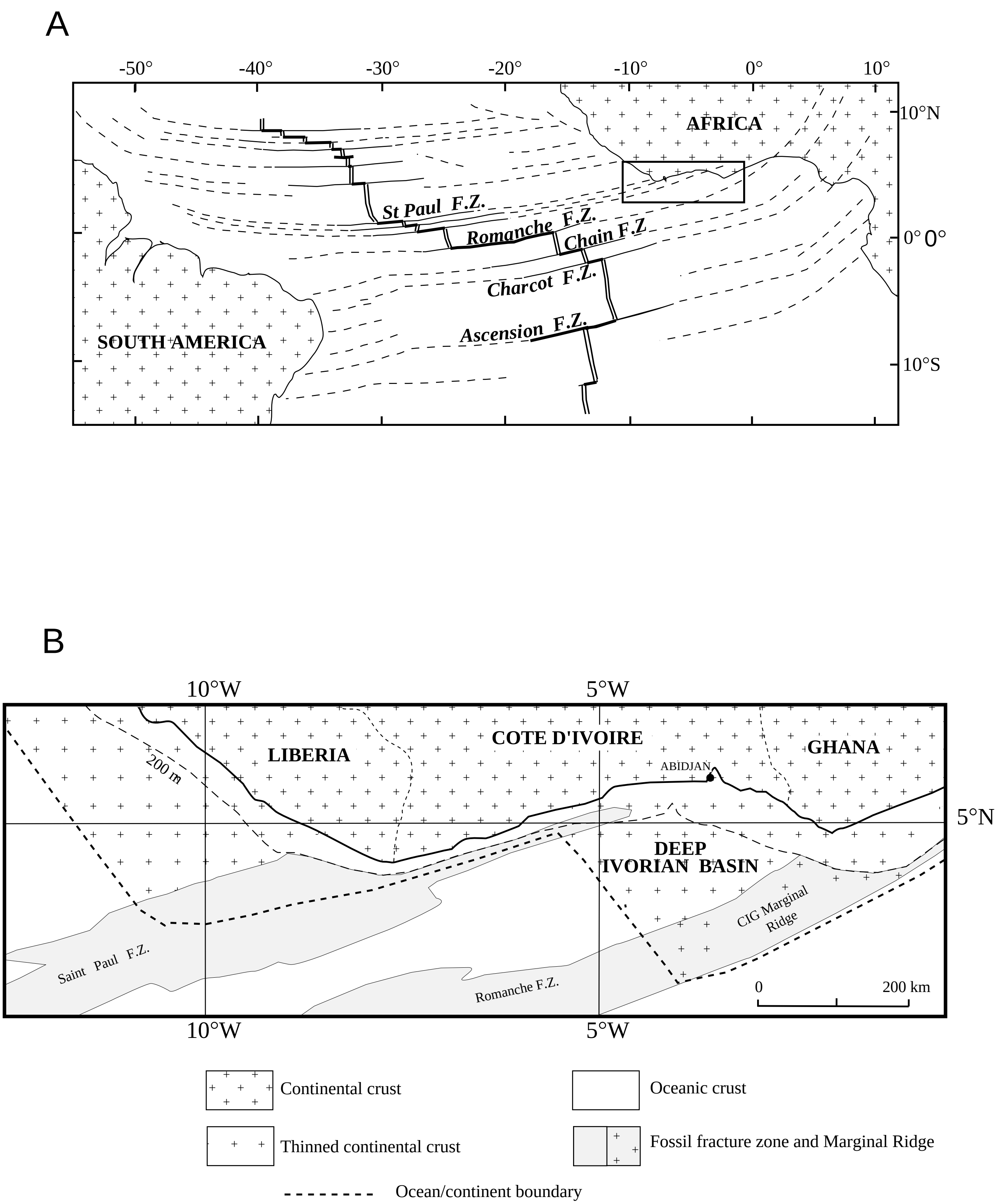
A
-50°
-40°
-30°
-20°
-10°
0°
10°
10°N
0°
10°S
AFRICA
SOUTH AMERICA
St Paul F.Z.
Romanche F.Z.
Chain F.Z
Charcot F.Z.
Ascension F.Z.
B
10°W
5°W
5°N
200 m
LIBERIA
COTE D'IVOIRE
GHANA
ABIDJAN
DEEP
IVORIAN BASIN
CIG Marginal
Ridge
Saint Paul F.Z.
Romanche F.Z.
0
200 km
Continental crust
Oceanic crust
Thinned continental crust
Fossil fracture zone and Marginal Ridge
Ocean/continent boundary

Figure 1

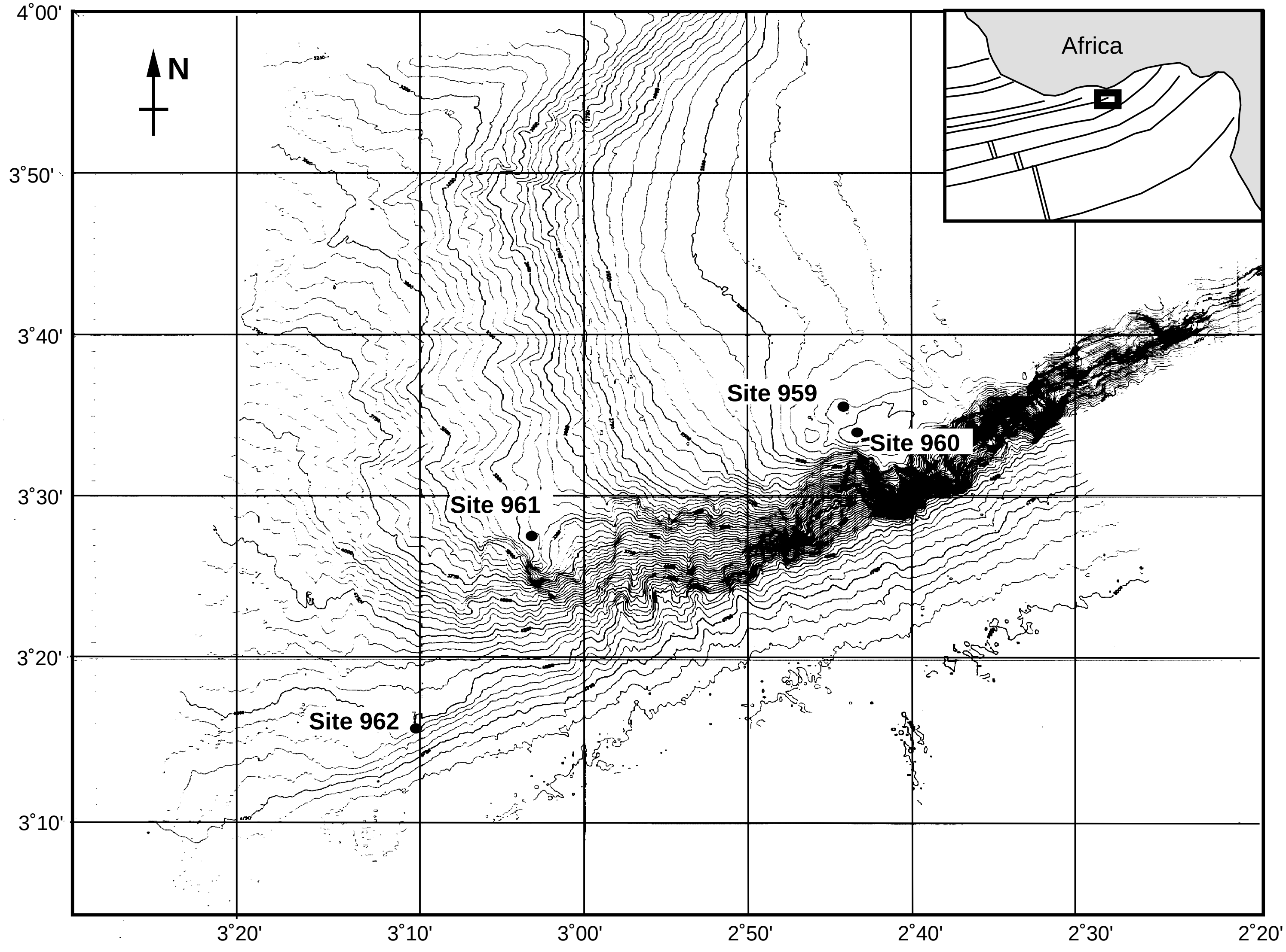
4˚00'
3˚50'
3˚40'
3˚30'
3˚20'
3˚10'
3˚20'
3˚10'
3˚00'
2˚50'
2˚40'
2˚30'
2˚20'
N
Africa
Site 959
Site 960
Site 961
Site 962

Figure 2

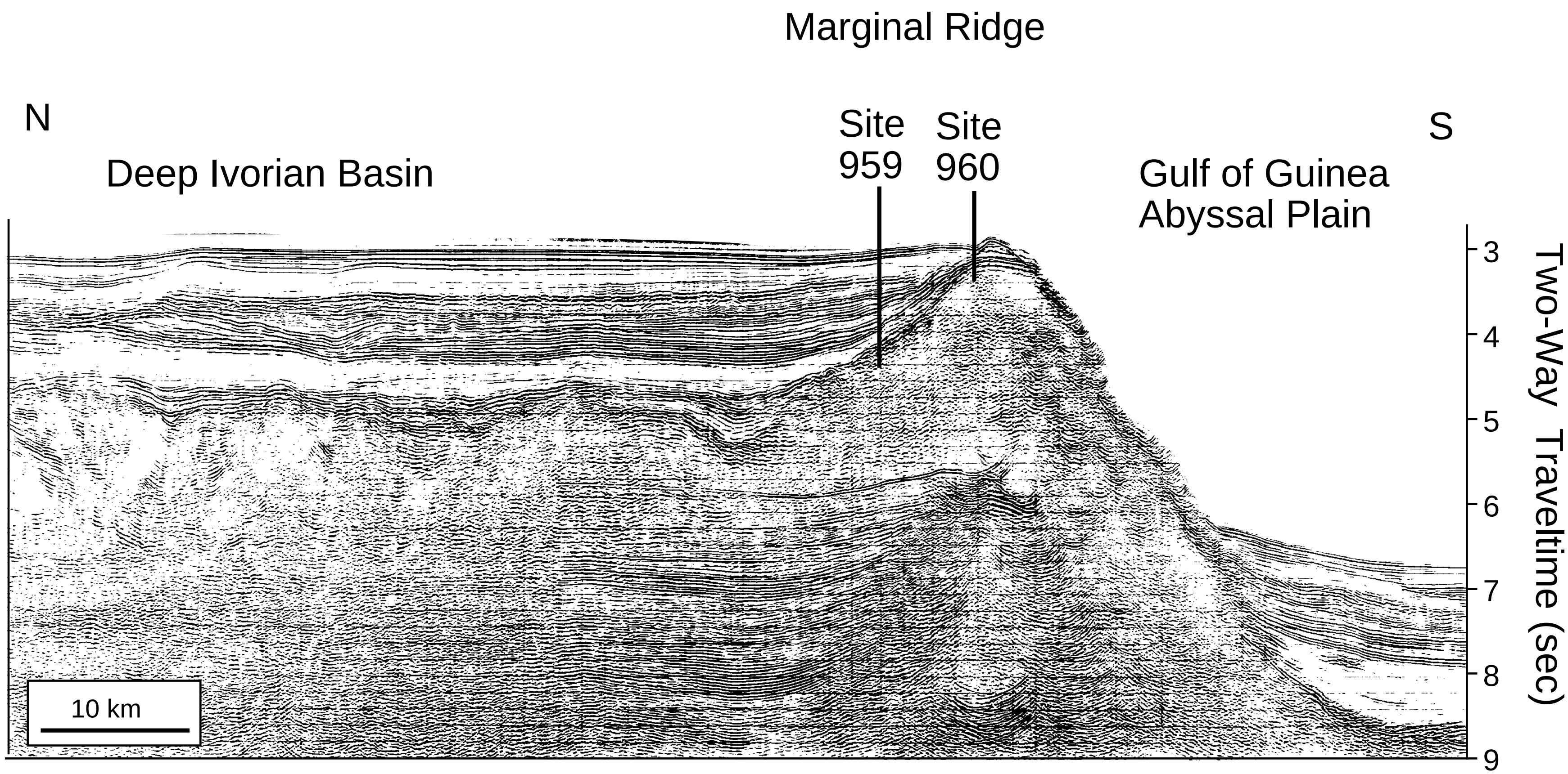
Marginal Ridge
N
Site 959
Site 960
S
Deep Ivorian Basin
Gulf of Guinea Abyssal Plain
3
4
5
6
7
8
9
Two-Way Traveltime (sec)
10 km

Figure 3

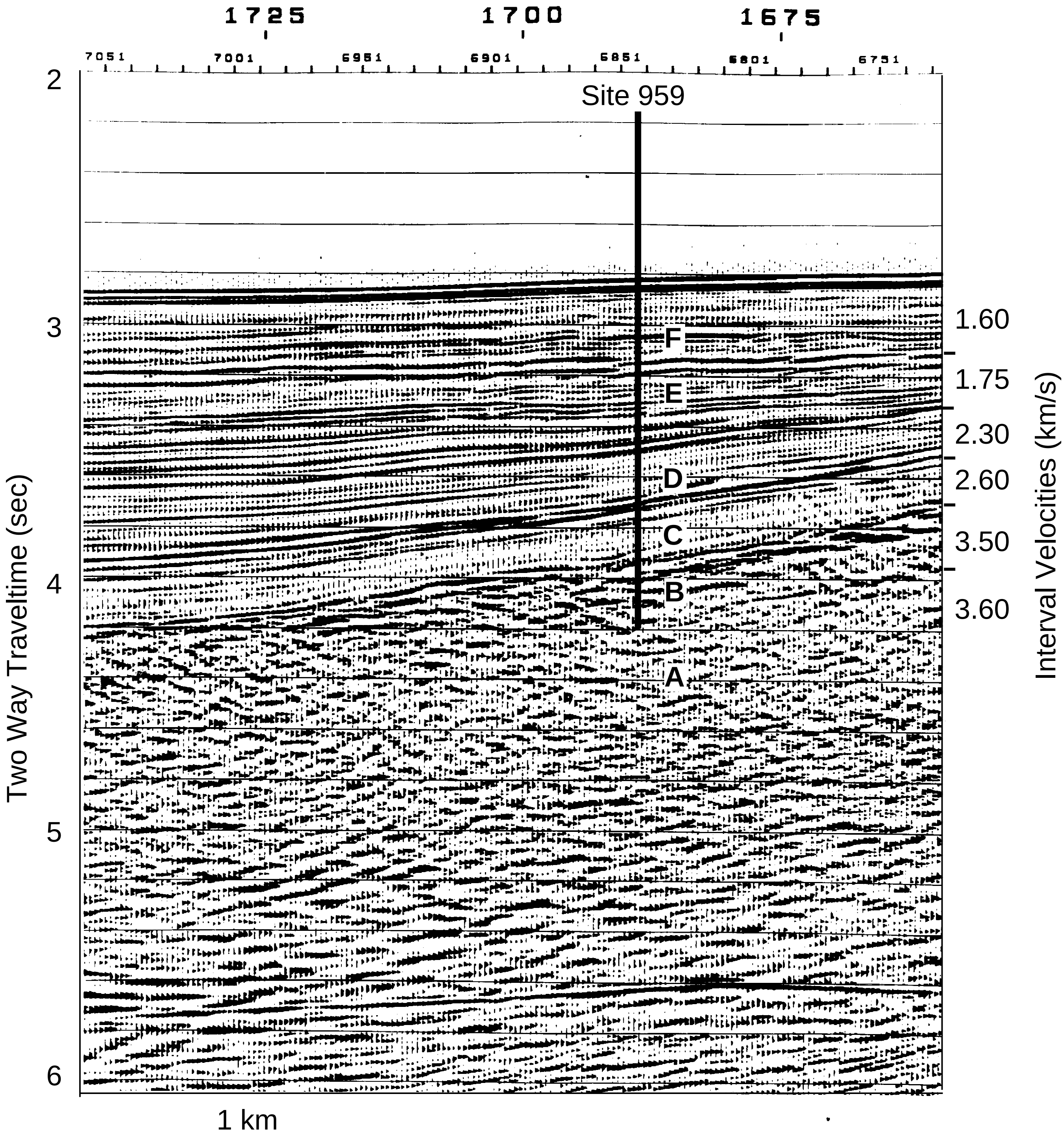
1725
1700
1675
7051
7001
6951
6901
6851
6801
6751
Site 959
2
3
4
5
6
Two Way Traveltime (sec)
F
E
D
C
B
A
1.60
1.75
2.30
2.60
3.50
3.60
Interval Velocities (km/s)
1 km

Figure 4

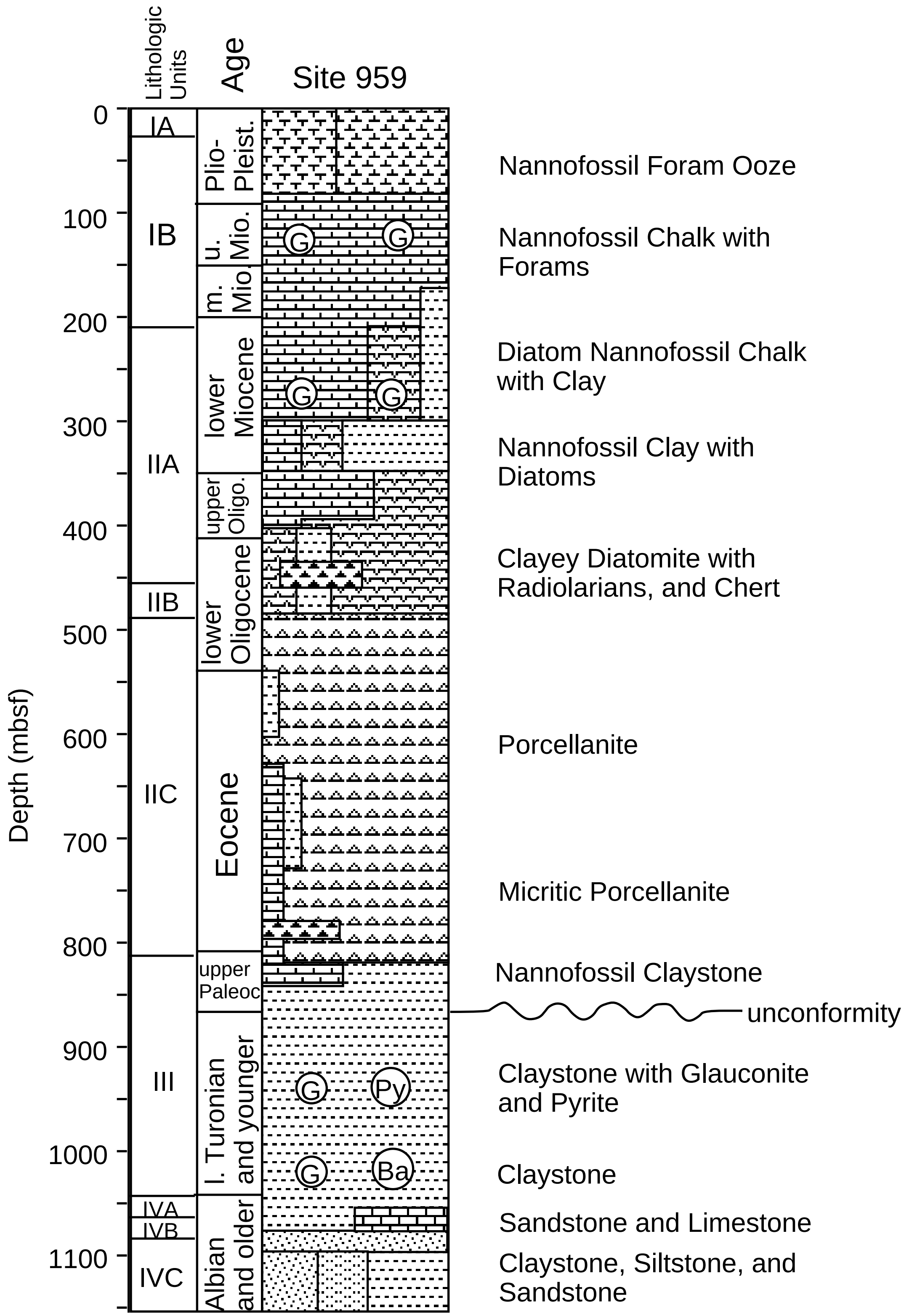
Lithologic Units
Age
Site 959
Depth (mbsf)
0
100
200
300
400
500
600
700
800
900
1000
1100
IA
IB
IIA
IIB
IIC
III
IVA
IVB
IVC
Plio-Pleist.
u. Mio.
m. Mio.
lower Miocene
upper Oligo.
lower Oligocene
Eocene
upper Paleoc
l. Turonian and younger
Albian and older
G
Py
Ba
Nannofossil Foram Ooze
Nannofossil Chalk with Forams
Diatom Nannofossil Chalk with Clay
Nannofossil Clay with Diatoms
Clayey Diatomite with Radiolarians, and Chert
Porcellanite
Micritic Porcellanite
Nannofossil Claystone
unconformity
Claystone with Glauconite and Pyrite
Claystone
Sandstone and Limestone
Claystone, Siltstone, and Sandstone

Figure 5

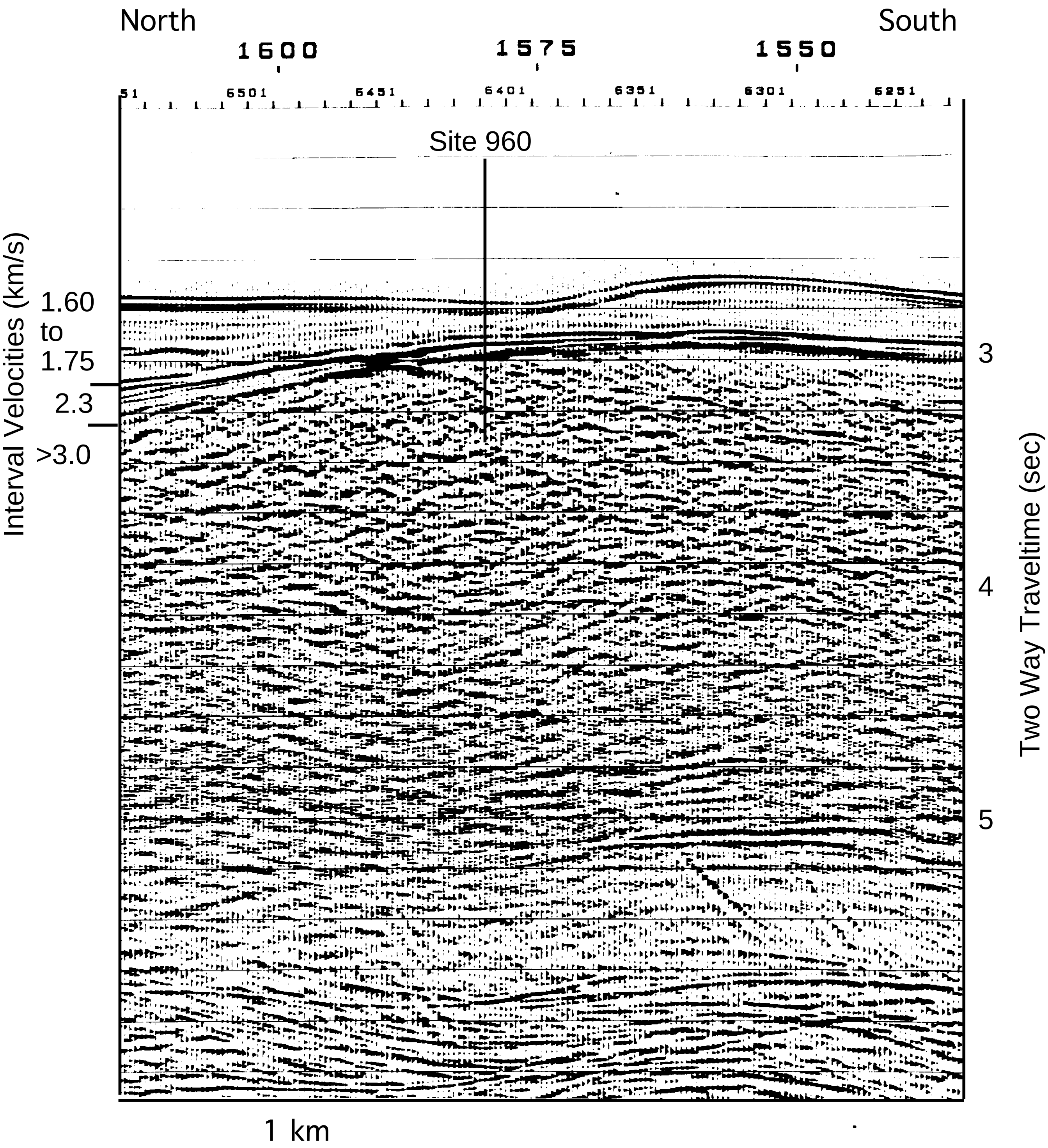
North
South
1600
1575
1550
6501
6451
6401
6351
6301
6251
Site 960
Interval Velocities (km/s)
1.60
to
1.75
2.3
>3.0
3
4
5
Two Way Traveltime (sec)
1 km

Figure 6

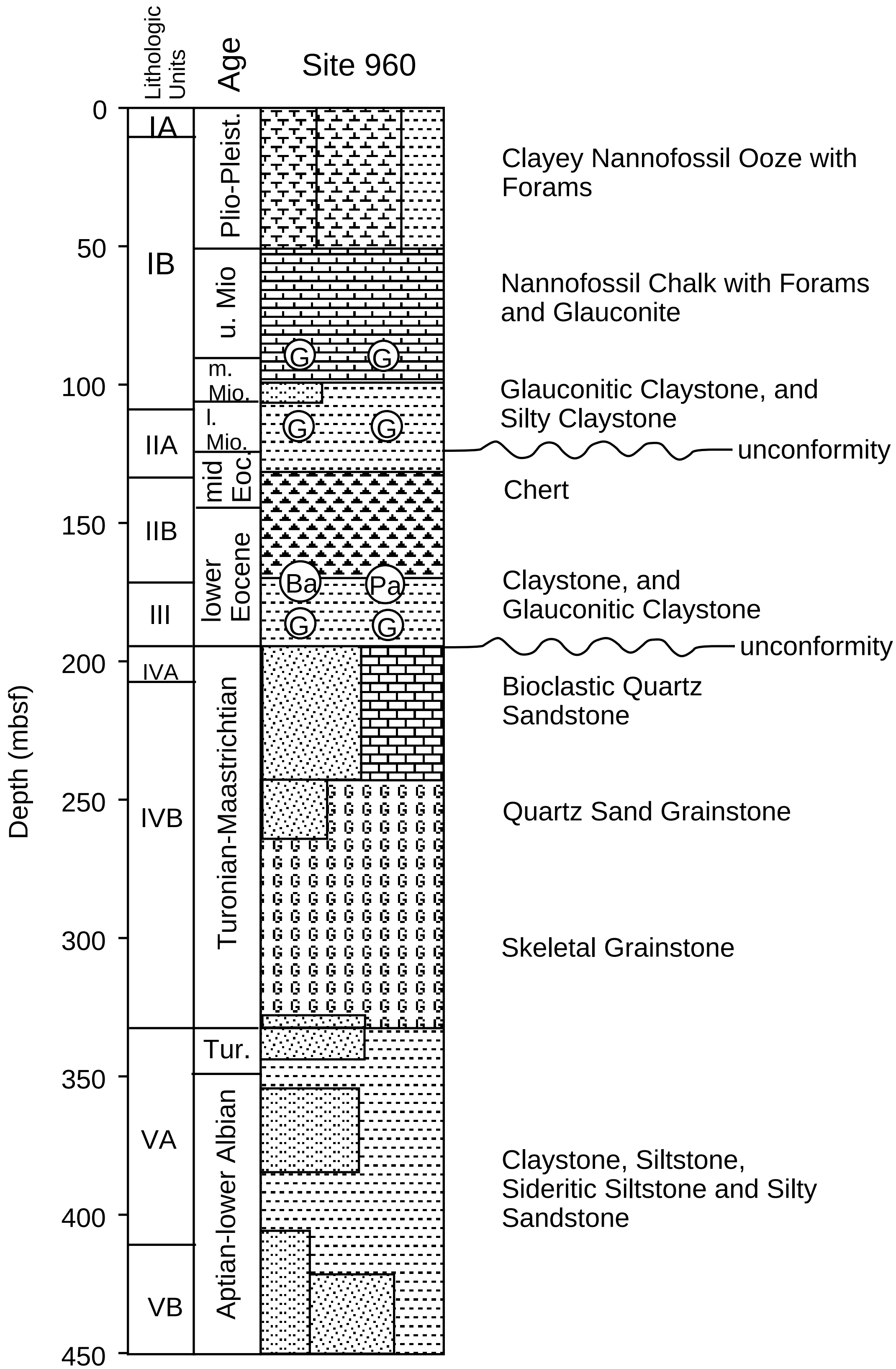
Lithologic Units
Age
Site 960
Depth (mbsf)
0
50
100
150
200
250
300
350
400
450
IA
IB
IIA
IIB
III
IVA
IVB
VA
VB
Plio-Pleist.
u. Mio
m. Mio.
l. Mio.
mid Eoc.
lower Eocene
Turonian-Maastrichtian
Tur.
Aptian-lower Albian
G
Ba
Pa
Clayey Nannofossil Ooze with Forams
Nannofossil Chalk with Forams and Glauconite
Glauconitic Claystone, and Silty Claystone
unconformity
Chert
Claystone, and Glauconitic Claystone
unconformity
Bioclastic Quartz Sandstone
Quartz Sand Grainstone
Skeletal Grainstone
Claystone, Siltstone, Sideritic Siltstone and Silty Sandstone

Figure 7

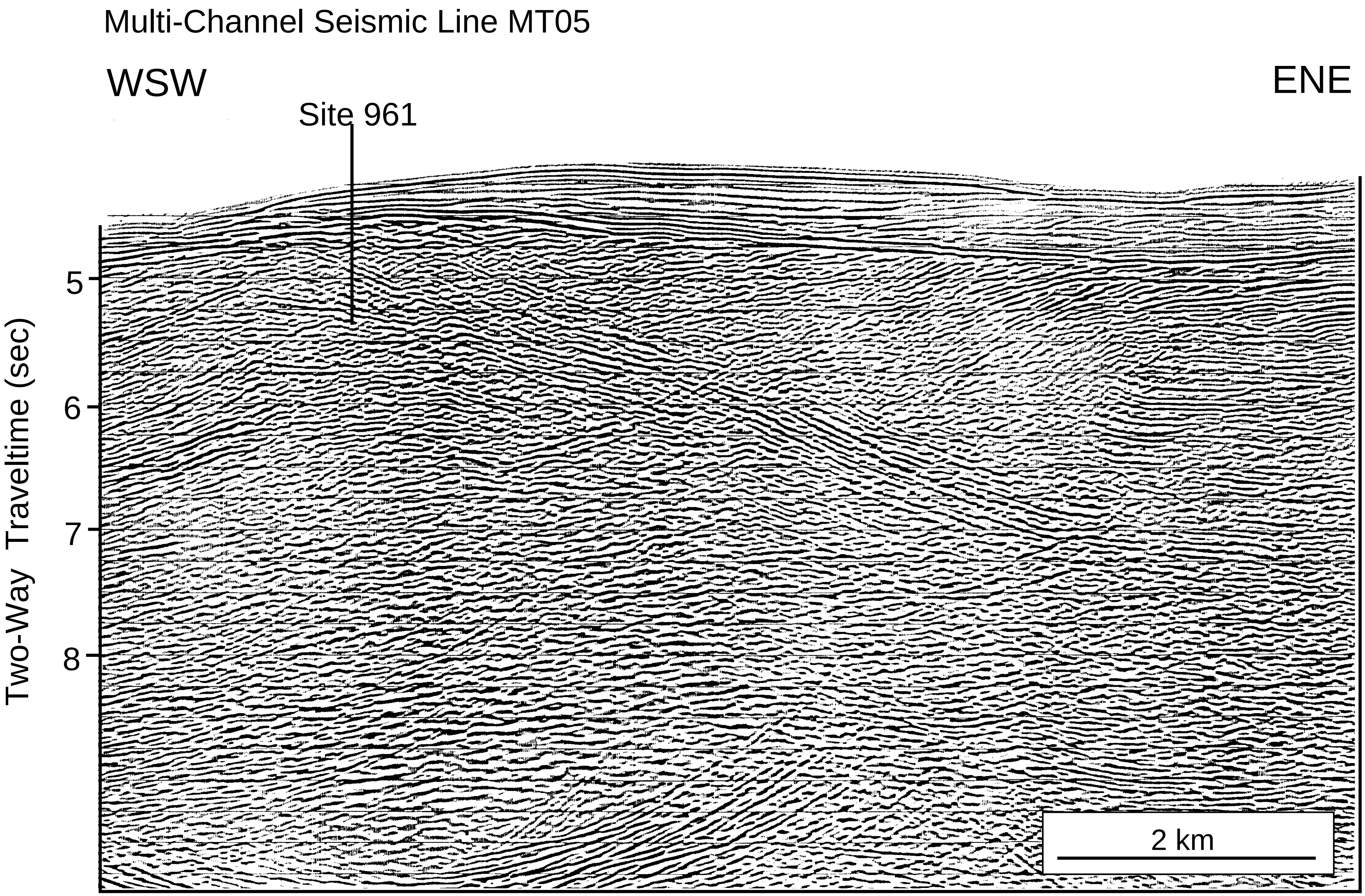

Multi-Channel Seismic Line MT05
WSW
ENE
Site 961
Two-Way Traveltime (sec)
5
6
7
8
2 km

Figure 8

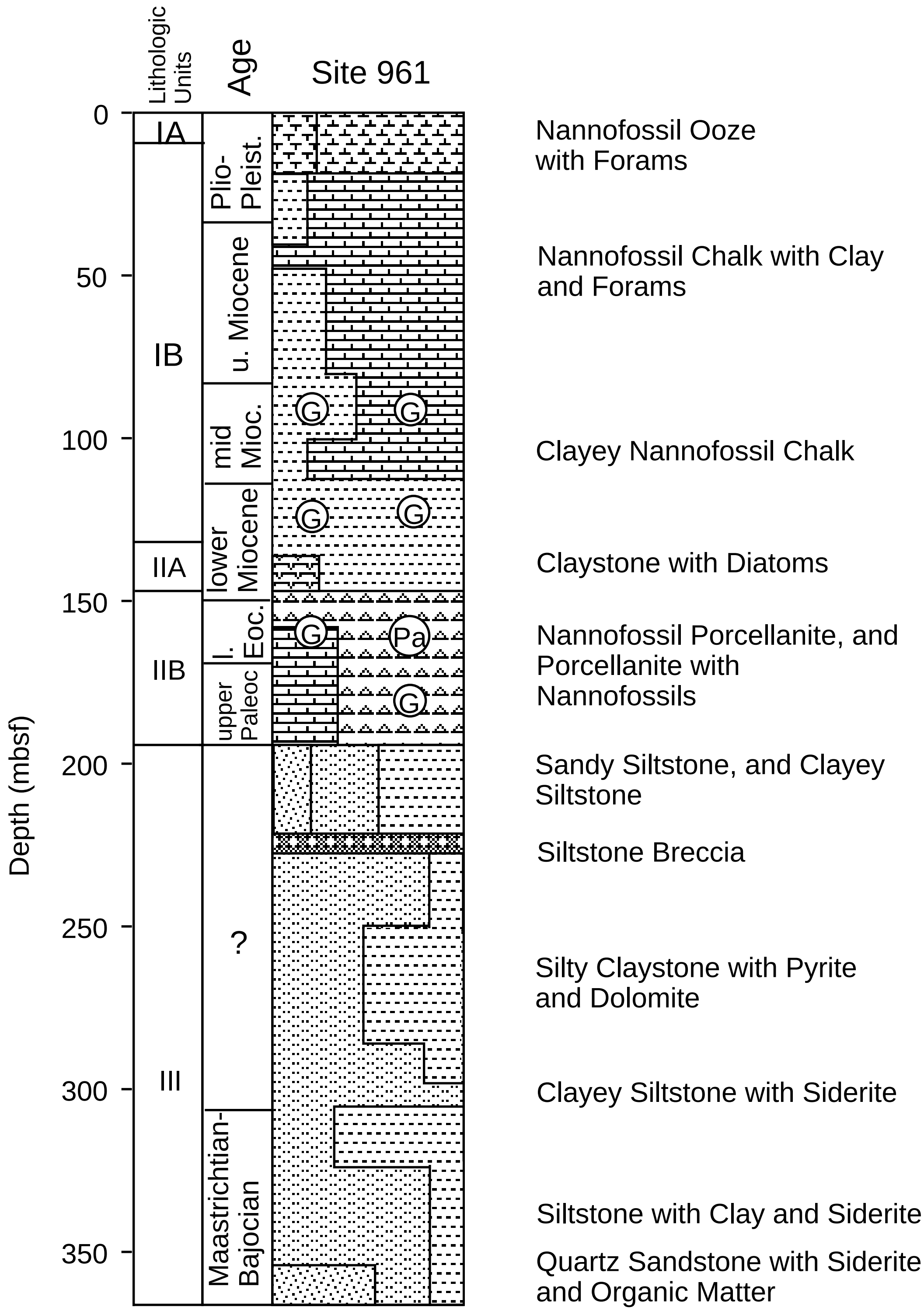
Lithologic Units
Age
Site 961
Depth (mbsf)
0
50
100
150
200
250
300
350
IA
IB
IIA
IIB
III
Plio-Pleist.
u. Miocene
mid Mioc.
lower Miocene
l. Eoc.
upper Paleoc
?
Maastrichtian-Bajocian
G
Pa
Nannofossil Ooze with Forams
Nannofossil Chalk with Clay and Forams
Clayey Nannofossil Chalk
Claystone with Diatoms
Nannofossil Porcellanite, and Porcellanite with Nannofossils
Sandy Siltstone, and Clayey Siltstone
Siltstone Breccia
Silty Claystone with Pyrite and Dolomite
Clayey Siltstone with Siderite
Siltstone with Clay and Siderite
Quartz Sandstone with Siderite and Organic Matter

Figure 9

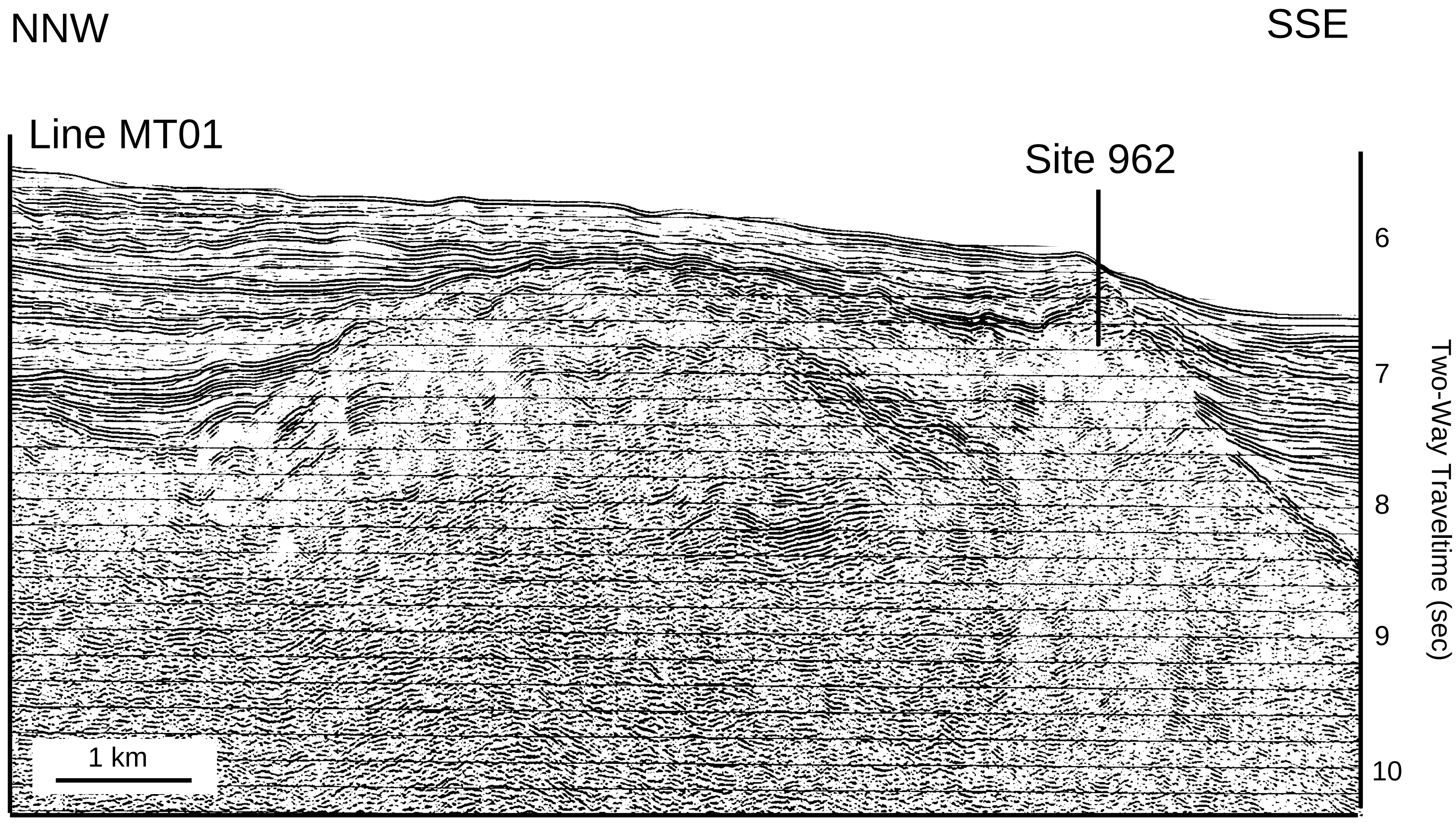

Figure 10

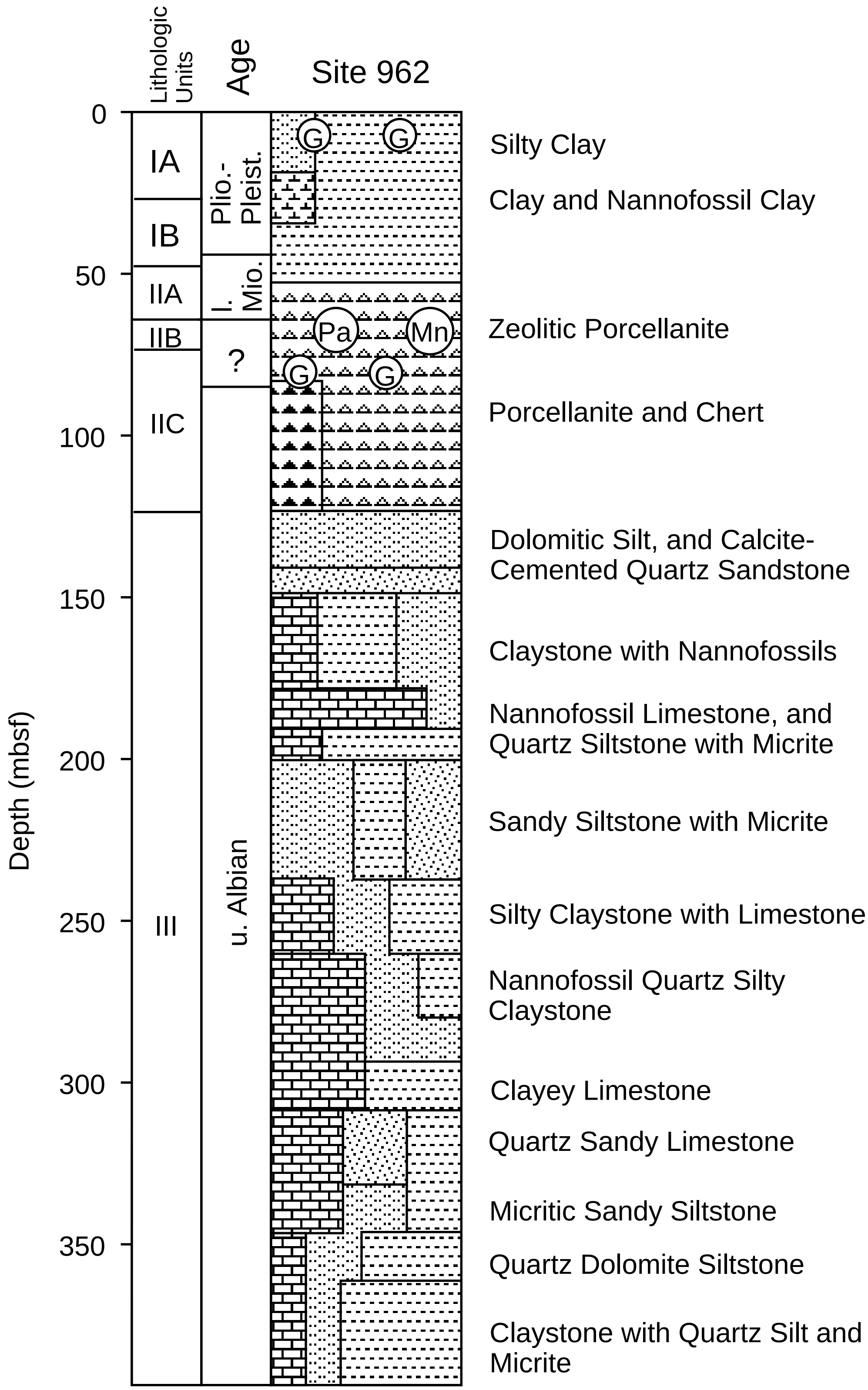
Lithologic Units
Age
Site 962
Depth (mbsf)
0
50
100
150
200
250
300
350
IA
IB
IIA
IIB
IIC
III
Plio.-Pleist.
l. Mio.
?
u. Albian
G
G
Pa
Mn
G
G
Silty Clay
Clay and Nannofossil Clay
Zeolitic Porcellanite
Porcellanite and Chert
Dolomitic Silt, and Calcite-Cemented Quartz Sandstone
Claystone with Nannofossils
Nannofossil Limestone, and Quartz Siltstone with Micrite
Sandy Siltstone with Micrite
Silty Claystone with Limestone
Nannofossil Quartz Silty Claystone
Clayey Limestone
Quartz Sandy Limestone
Micritic Sandy Siltstone
Quartz Dolomite Siltstone
Claystone with Quartz Silt and Micrite

Figure 11

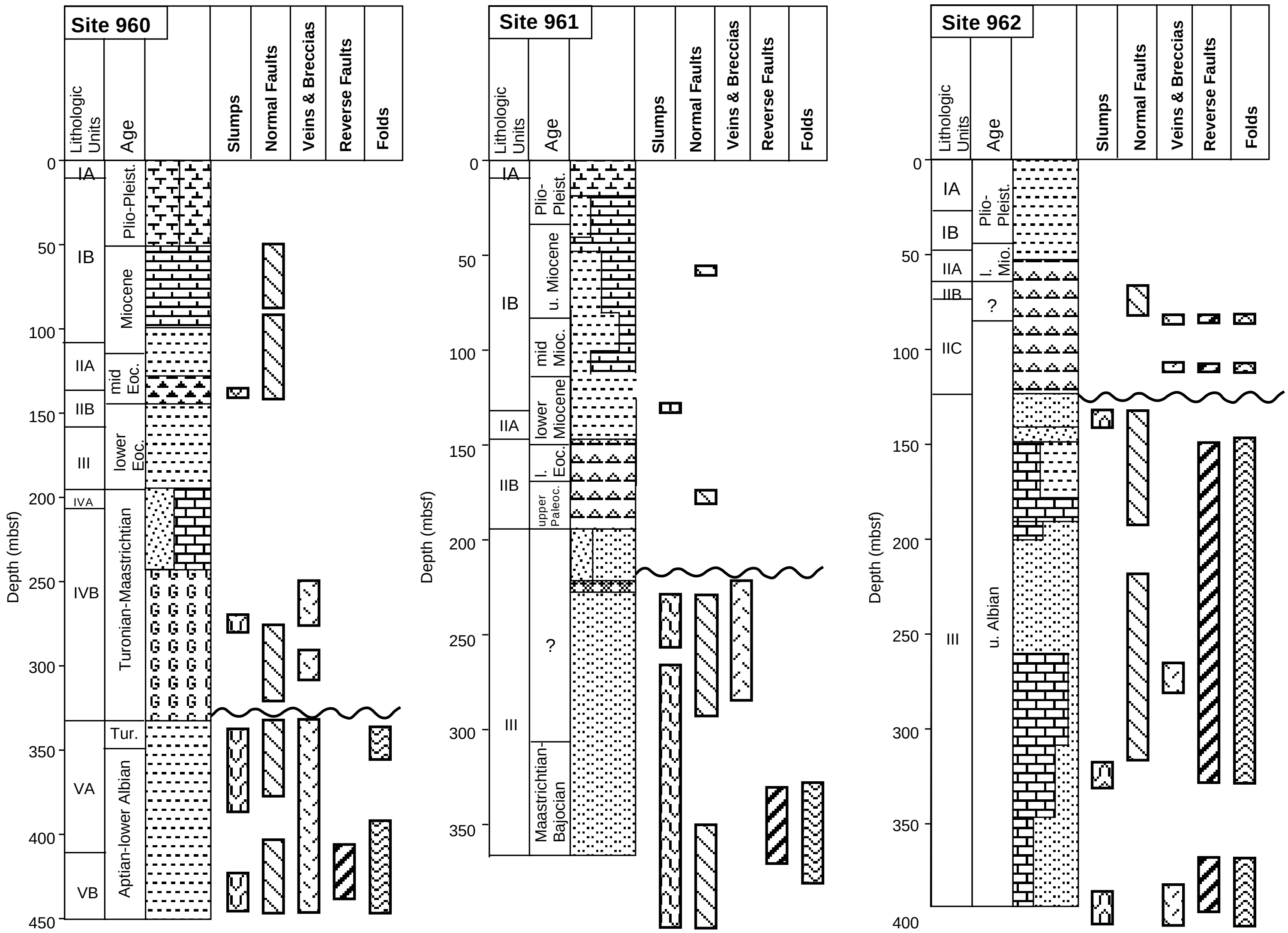
Site 960
Lithologic Units
Age
Slumps
Normal Faults
Veins & Breccias
Reverse Faults
Folds
Depth (mbsf)
IA
IB
IIA
IIB
III
IVA
IVB
VA
VB
Plio-Pleist.
Miocene
mid Eoc.
lower Eoc.
Turonian-Maastrichtian
Tur.
Aptian-lower Albian
Site 961
IA
IB
IIA
IIB
III
Plio-Pleist.
u. Miocene
mid Mioc.
lower Miocene
l. Eoc.
upper Paleoc.
?
Maastrichtian-Bajocian
Site 962
IA
IB
IIA
IIB
IIC
III
Plio-Pleist.
l. Mio.
?
u. Albian

Figure 12

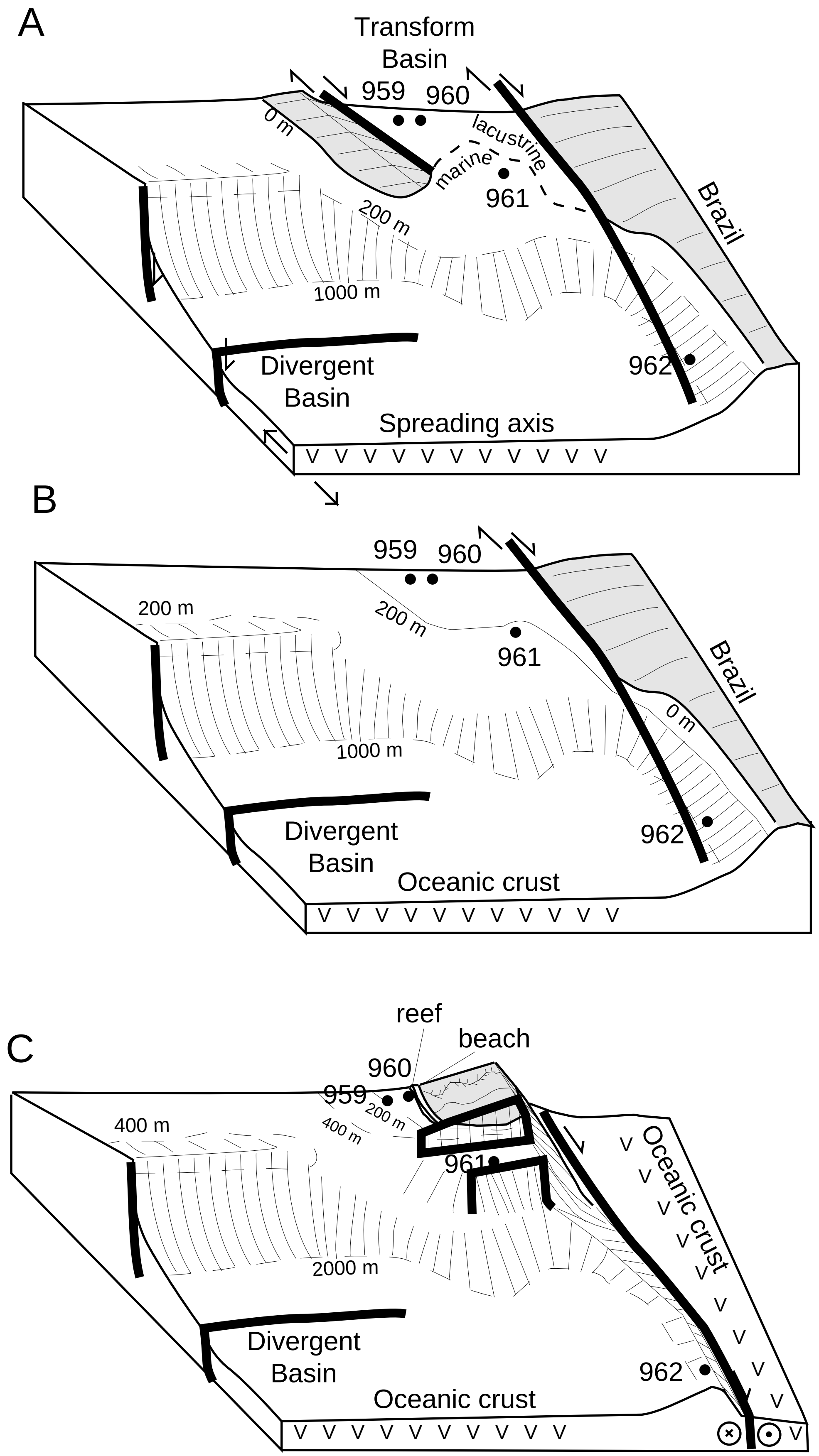
A
Transform
Basin
959
960
0 m
lacustrine
marine
961
Brazil
200 m
1000 m
962
Divergent
Basin
Spreading axis
B
959
960
200 m
200 m
961
Brazil
0 m
1000 m
962
Divergent
Basin
Oceanic crust
C
reef
beach
960
959
400 m
200 m
400 m
961
Oceanic crust
2000 m
962
Divergent
Basin
Oceanic crust

Figure 13

OPERATIONS REPORT

The ODP Operations and Engineering personnel aboard *JOIDES Resolution* for Leg 159 were:

Operations Manager:Michael Storms

Schlumberger Wireline Logging Engineer:Richard Sammy

PORT CALL, DAKAR, SENEGAL

ODP Leg 159 began when *JOIDES Resolution* arrived dockside in Dakar, Senegal, at 0700 hr, 3 January 1995 (all times local). Since the vessel had just completed a dry-docking period in Falmouth, England, there were no logistical or repair activities to be accomplished in Dakar. All resupply was handled in Falmouth, limiting Dakar activities to technical crew change and the boarding of the scientific party. All personnel were aboard ship by 1200 hr, 4 January 1995. Sailing clearances were obtained and the last line was away at 1430 hr. Once clear of the Dakar breakwater, the captain set a southeasterly course for Site 959 (proposed site IG-1).

TRANSIT FROM DAKAR TO SITE 959
(Proposed site IG-1)

Having a newly cleaned hull and favorable weather conditions, *JOIDES Resolution* made excellent time en route to the operating area for Site 959 (proposed site IG-1). The Guinea Current, flowing southeasterly off the west coast of Africa, at a speed of up to 1.5 kt, helped the vessel to achieve an average speed of 13.2 kt for the transit. Due to recent articles describing an increase in piracy off the west coast of Africa, the vessel kept 35-40 nmi away from the coastline while transiting to the operating area.

While en route to the operating area, we decided to spend up to 24 hr conducting a pre-site seismic survey of all three primary drill sites (proposed sites IG-1, IG-2, and IG-3) and to pre-deploy positioning beacons at each site. The waypoint for the start of surveying activities was reached at 1600 hr, 8 January 1995. Approximately 8 hr was spent conducting a 3.5-kHz single channel seismic survey of each primary proposed drill site. A duplication of the original pre-cruise survey line across each site was accomplished in addition to a second, roughly perpendicular, crossing line to aid in locating the site as accurately as possible. The possibility of a hydrocarbon risk in this area made the accurate positioning of the drill sites, using the pre-cruise multichannel seismic survey, imperative. Our survey aimed to reproduce the previously revealed structure and permit accurate location of the sites.

At 0045 hr, 9 January 1995, beacon SN 1242 (Datasonics Model 354B, 15 kHz, 208 dB) was deployed at Site 962 (proposed site IG-3). At 0945 hr that same day, beacon SN 1248 (Datasonics Model 354B, 14.5 kHz, 208 dB) was deployed at Site 961 (proposed site IG-2). After completion of the 3.5-kHz seismic survey of the “IG” operating area, the last beacon (Datasonics Model 354B, 15 kHz, 208 dB, SN 779) was dropped on location at 1630 hr, January 9, at Site 959 (proposed site IG-1).

SITE 959
(Proposed site IG-1)

Site 959 lies on the continental slope off the southwest coast of Ghana, approximately 130 nmi southeast of Abidjan in 2100 m of water. Initial plans called for multiple holes at this site beginning with triple advanced hydraulic piston coring (APC) to approximately 200 mbsf, or to APC refusal. The third APC hole was to be deepened to approximately 300 mbsf or greater if the extended core barrel (XCB) coring system was yielding satisfactory results. The APC/XCB coring was to be followed by a single bit rotary core barrel (RCB) hole to a depth of approximately 900 mbsf, or until a satisfactory casing point was located for the deep coring effort on the following hole. The final hole at this site was projected to be cored to a final depth of 1600 mbsf. To accomplish this, it was anticipated that a full reentry cone installation, including a 10-3/4-in. surface casing string to approximately 870 mbsf, would be required.

Hole 959A

The APC/XCB bottom hole assembly (BHA) was made-up with a non-magnetic drill collar and a new Security 11-7/16-in. S86F bit (SN 479055). The BHA was run in the hole at 0100 hr, 10 January. The first APC core was shot from a depth of 2101.0 m. The mud line was established at 2102.0 m (according to the direct pipe measurement, DPM). The corrected precision depth recorder (PDR) reading normalized to driller's datum was 2106.4 m (according to the PDR). APC coring advanced through a greenish gray nannofossil ooze to a refusal depth of 180.1 mbsf (Core 159-959A-19H). The APC cored section recovered 188.69 m or 104.3% of the interval cored. The cores were oriented beginning with Core 159-959A-3H, and three successful Adara temperature tool measurements were taken at 85.1 mbsf (Core 159-959A-9H), 132.6 mbsf (Core 159-959A-14H), and 180.1 mbsf (Core 159-959A-19H), respectively. Data from the first Adara temperature measurement, attempted at a depth of 37.6 m (Core 159-959A-4H) was considered suspect due to apparent movement of the cutting shoe.

The XCB was then deployed to give the scientific party the opportunity to evaluate the quality of the piston cores from Hole 959A before APC coring resumed at Holes 959B and 959C. During XCB coring, a second positioning beacon was deployed as a back-up to the primary beacon. At 2025 hr, 10 January, beacon SN 1245 (Datasonics Model 354B, 17 kHz, 208 dB) was deployed. When this beacon would not command off at the seafloor, the primary (initial) beacon was turned off and positioning continued using the back-up beacon for the remainder of the site. The XCB core barrel was dropped, and XCB coring advanced from 180.1 to 479.9 mbsf. The cored interval was 299.8 m, with 267.51 m recovered (89.2%).

Hydrocarbons

Gas chromatograph (GC3) and Natural Gas Analyzer (NGA) analysis on Core 159-959A-50X indicated the presence of long-chain hydrocarbons up to C_6 and higher. The data suggesting the presence of long-chain hydrocarbons in Core 159-959A-50X were considered suspect for several reasons. Normal trends associated with the approach to a hydrocarbon reservoir were absent. Unusual chemical bonding, as well as a variety of complex and substituted hydrocarbon chains, was prevalent, indicating a non-equilibrium environment. This was considered inconsistent with the normal occurrence of hydrocarbons and more likely to indicate a recent, artificially induced, phenomenon. A burnt smell associated with the XCB cutting shoes was noticed in Cores 159-959A-49X to -51X. Levels of total organic carbon (TOC) were identified in the sediments sufficient to yield higher long-chain hydrocarbons if adequate heat was applied. It was therefore suggested that the long-chain hydrocarbons were produced as a result of extreme frictional heating by the XCB cutting shoes during the coring process. To confirm this theory a single APC core (Core 159-959A-52H) was taken to a depth of 480.7 mbsf as the last core of the hole. The APC advanced 0.8 m, and recovered 0.74 m. Headspace analysis of the core indicated that the hole was within acceptable hydrocarbon limits. A methane/ethane ratio of 1120/1 was established, and, on three of four samples, there was no detectable ethane. No hydrocarbons above C_3 were identified.

Hole 959A was terminated at a depth of 480.7 mbsf due to poor recovery with the XCB coring system and in favor of spudding the scheduled single bit RCB hole to reach the deeper objectives. In total, the APC/XCB coring systems recovered 456.20 m or 94.9% of the section cored on Hole 959A. The bit cleared the seafloor at 1215 hr, 12 January, ending Hole 959A.

Hole 959B

Hole 959B was spudded at 1300 hr, 12 January, after offsetting the vessel 15 m due north of Hole 959A. The first APC core was shot from a depth of 2097.0 m to stagger the cored interval from Hole 959A. The mud line was established at 2101.5 m (DPM). APC coring advanced through the same greenish gray nannofossil ooze as cored in Hole 959A until reaching a refusal depth of 184.4 mbsf (Core 159-959B-20H). The APC-cored section recovered 192.53 m or 104.4% of the interval penetrated. The cores were oriented beginning with Core 159-959B-3H and successful Adara temperature measurements were taken at depths of 43.0 mbsf (Core 159-959B-5H), 81.0 mbsf (Core 159-959B-9H), and 138.0 mbsf (Core 159-959B-15H). At 0315 hr, 13 January, the bit cleared the seafloor, ending Hole 959B.

Jet-in Test

Prior to spudding Hole 959C, the vessel was offset 15 m north and 30 m east of Hole 959B. This was the planned location for the reentry cone installation for Hole 959E. A successful jet-in test was conducted to aid in establishing the amount of 16-in. casing to be made-up to the reentry cone. Jet-in testing lasted 1 hr and penetrated to a depth of 72 mbsf, using up to 40 strokes per min (spm).

Hole 959C

Hole 959C was spudded at 0630 hr, 13 January, after offsetting the vessel 30 m west of the jet-in location, which corresponds to a location 15 m north of Hole 959B. The first APC core was shot from a depth of 2094.0 m to stagger the cored interval from Holes 959A and 959B. The mud line was established at 2101.2 m (DPM). APC coring advanced until reaching a refusal depth of 179.6 mbsf (Core 159-959C-20H). The APC-cored section recovered 187.34 m or 104.3% of the interval cored. As in the two previous holes, the cores were oriented beginning with Core 159-959C-3H. There were no Adara temperature measurements attempted in this hole. Upon completing the third set of APC coring, the drill string was tripped back to the drill floor of the ship so that the APC/XCB BHA could be changed over to that required for rotary (RCB) coring. At 2400 hr, 13 January, the bit cleared the rig floor, ending Hole 959C.

Hole 959D

While making-up an RCB BHA and mechanical bit release, the vessel was offset 60 m south and 30 m west of Hole 959C. This placed Hole 959D to the south and west of Holes 959A and 959C. Reentry Hole 959E was planned for spudding to the northeast, thus maximizing the separation between the site's two projected deepest holes, 900 m and 1600 m, respectively. The RCB wireline core barrels were spaced out, and the drill string was run in the hole. Hole 959D was spudded with a center bit in place at 0645 hr, 14 January. Since Hole 959A was located within 30 m of Hole 959D, the water depth (2102 m DPM) from that hole was used in this case as well. After drilling ahead for 11.75 hr at an average rate of penetration (ROP) of 38 m/hr, the center bit barrel was recovered and an RCB core barrel was pumped to bottom. Continuous RCB coring was initiated at 1830 hr, 14 January, at a depth of 417.8 mbsf, approximately 63 m above the depth at which APC/XCB coring was terminated in Hole 959A. Although it was hoped that the RCB coring system would get better recovery through this interval than the XCB system, this proved not to be the case. Since this interval was also an area of concern due to the hydrocarbon indications in Hole 959A, particular attention was paid to the headspace analysis of the RCB cores as the hole approached the termination depth of Hole 959A. No hydrocarbons higher than C_3 were identified, and even these were in trace amounts. Methane/ethane ratios were also well within accepted limits.

This seemed to confirm the idea that high temperatures generated from XCB cutting shoes during the coring process caused artificial hydrocarbon indications.

When Hole 959D reached the target depth of 900 mbsf, a wiper trip was made with the drill string to 100 mbsf, and showed that hole stability was excellent. There was no evidence of fill, drag, overpull, abnormal torque, or pump pressure to indicate any existing or impending downhole problem. No rotation of the pipe was required during the trip; however, after the trip, there was 15 m of debris at the bottom of the hole. The decision was made to continue coring ahead. Core recovery and ROP were excellent. It was theorized that if Hole 959D could be deepened to the target stratigraphic depth (approximately 1600 mbsf), then that would eliminate the need for setting a reentry cone and 10-3/4-in. surface casing string. This, in turn, would save a great deal of hardware and a significant amount of operating time. Should the depth objective of 1600 mbsf not be reached in this hole, then it was planned to recover the lowermost part of the section at a second site, proposed site IG-1bis, the planned alternate to IG-1 (Site 960). This plan optimized the potential scientific return by maximizing coring time and also allowed a larger quantity of the deepest sediments (seismic unit A) to be cored rather than spending a long time coring the overlying relatively thick (450 m) sediments of seismic unit B.

As depth of the hole increased beyond 1000 mbsf, coring was interrupted on several occasions to wait for hydrocarbon analysis. The black shale sediments then being cored tended to yield peaks in the hydrocarbon analysis with the levels dropping off dramatically in sandstone interbeds. Below Core 159-959D-64R (1024.1 mbsf), higher hydrocarbons (NC4 to IC5) were detected in trace amounts. Cores 159-959D-65R (1033.7 mbsf) and -66R (1043.3 mbsf) had 6 and 10 ppm C_6 respectively, with 6.6% methane and a methane/ethane ratio of 82:1. Analysis of Core 159-959D-67R (1053.0 mbsf) was more favorable, and yielded only 0.59% to 0.88% methane and a ratio of 40:1. The quantity of NC4 and IC5 dropped by 66%, and no C_6 was detected.

RCB coring continued for 6 days, with recovery reaching an average of 57.9%. Recovery of black shales and siltstones was excellent, even exceeding 100% at times. This was tempered by poor recovery (<10%) in the fractured sandstones and in areas where chert was present. As far downhole as 745 mbsf, penetration rates were surprisingly good, and ranged from 19 to 38 m/hr. Zones of accelerated penetration rate (6-7 min/core) and minimal recovery (3%-6%) at 450-480 mbsf were associated with chert recovery.

Hole 959D was terminated at 1158.9 mbsf due to increasingly poor ROP and the continued occurrence of thick black shale intervals with associated hydrocarbon spikes. Headspace analysis on Core 159-959D-78R yielded a C_1/C_2 ratio of 30, the same as Core 159-959D-77R. Ethane was measured at only 3%, while C_3, NC4, and IC4 were present in trace amounts. No higher hydrocarbon chains were present. The hydrocarbon situation had minimal impact on the decision to terminate Hole 959D. Instead, the major scientific objectives had been accomplished, and, since the ROP had been steadily decreasing (Core 159-959D-78R took 200 min to cut 9.7 m of unconsolidated black shale), it was decided that the remaining objectives would likely be better attained at the alternate proposed site IG-1bis.

Logging Operations

After termination of the drilling effort, a 30-bbl sepiolite mud pill was circulated from the bottom up and a second wiper trip was made to 100 mbsf. The second wiper trip went as well as the first. Hole stability continued to be excellent, and there was no evidence to indicate any existing or impending downhole problem. Two wireline runs were made to release the mechanical bit release (MBR) and subsequently shift the sleeve back down to close off the dog windows in the side of the MBR top connector. The hole was displaced with 400 bbl of sepiolite mud, and the pipe was tripped to 99.5 mbsf in preparation for logging operations. Due to the anticipated hole conditions, the conical side entry sub (CSES) was not picked-up.

After rigging the Schlumberger logging sheaves, the first suite of tools was assembled. Run no. 1, referred to as the quad combo, was run into the hole, but was only able to reach 120 mbsf, or approximately 20 m below the end of the pipe. It was suggested that the sticky clays recovered in this portion of the hole were swelling due to hydration and causing a blockage problem. The logging tools were recovered and the CSES was picked-up to allow the drill pipe to be lowered past the restriction. The drill string was lowered to 390 mbsf before encountering a restriction, which proved impassable without the ability to rotate the pipe. Because the logs in the lower portion of the hole were of the top priority, the pipe was tripped back, the CSES was removed, and the top drive was picked-up. With rotation, the string was lowered to 423 mbsf and the quad combo logging string was run into the hole, before stopping at 548 mbsf, or 125 m beyond the end of the pipe. This portion of the hole was then logged.

All indications were that the hole remained in good condition, as the drill pipe was not encountering any drag or resistance during the lowering process. Because of this, it was theorized that the hole might be slightly deviated from the vertical and have a rugose wall due to the interbedded formations. Lack of centralization of the logging tools would allow them to lie on the low side of the hole and tend to hang up on downhole ledges. To try and circumvent this problem, a meter-long rubber “hole finder” was installed on the bottom of the logging suite in place of the LDEO temperature tool. After recovering the logging tools, the top drive was again picked up and the pipe was run farther into the hole to a depth of 567 mbsf. The top drive was set back and the second run (run no. 2) with the quad combo tools was made. This time a depth of 1081 mbsf was reached, within 78 m of the total depth of the hole. Logs were obtained from this interval up to the pipe at 567 mbsf. The next logging run (run no. 3) was made with the FMS and natural gamma tool (FMS/NGT). These tools reached a depth of 938 mbsf, and logs were obtained from that depth up to the drill pipe at 538 mbsf. The final logging run (run no. 4) was made with the geochemical tool (GST, ACT, CNTG, and NGTC). These tools reached a depth of 927 mbsf, and logs were obtained from that point up to the drill pipe at 538 mbsf. This concluded logging operations for Hole 959D. After rigging down the last suite of tools and the logging sheaves, preparations were begun for the plugging and abandonment of the hole.

Plugging and Abandonment

Because Hole 959D was located on a continental slope, the hole was filled with 117 bbl of 10 ppg weighted mud and capped with a 20 bbl cement plug. The drill string was pulled out of the hole, and, after clearing the mud line, the pipe was flushed with seawater to remove any residual cement. During the trip, the primary and back-up positioning beacons were commanded to release. The primary beacon (SN 779) was recovered in short order; however, the back-up beacon (SN 1245) apparently failed to release and was not observed at the surface. Tripping of the drill string was then resumed, and the MBR top connector reached the rig floor at 0530 hr, thus completing Hole 959D.

TRANSIT TO SITE 960
(Proposed site IG-1bis)

The transit to Site 960 from Site 959 was made in dynamic positioning (DP) mode due to the short distance (2.7 nmi) between the two sites. No site survey was required, and the site, which was originally planned as an alternate to Site 959, was located using the GPS navigation system. Once the drill string was clear of the seafloor at Site 959, and the positioning beacon had been recovered, the vessel began moving to Site 960.

SITE 960
(Proposed site IG-1bis)

The BHA for Hole 960A was the same as that used in Hole 959D. As the vessel arrived on location, the BHA was being assembled, and RCB's were spaced out. The same positioning beacon (Datasonics Model 354B, 15 kHz, 208 dB, SN 779) that was recovered from Site 959 was deployed, thus initiating Hole 960A at 0630 hr, 24 January.

Hole 960A

The RCB BHA was run in the hole, and, at 1200 hr, 24 January, Hole 960A was spudded, with the mud line being established at 2059.7 m by DPM. The corrected precision depth recorder (PDR) reading normalized to driller's datum was 2048.4 m. The discrepancy was attributed to the difficulty in "feeling" for bottom with the drill pipe and RCB core bit. RCB coring continued at a fairly rapid rate in the upper, softer sediments; however, recovery varied erratically, averaging less than 30% for the first 280 mbsf. The presence of poorly consolidated nannofossil oozes and claystones, followed by hard cherts and weakly cemented limestones, was believed to be the primary contributor to the core recovery problems. The condition of the hole was excellent.

At approximately 2394 m drill pipe depth (334 mbsf) in Core 159-960A-37R, the contact between seismically defined units A and B was recovered. Recovery was surprisingly good in the sandstone/shale interbeds below this contact, with two black shale cores recovering 99%. The rate of penetration continued to deteriorate, however, ranging from 0.7 to 1.4 m/hr. Although core diameter and recovery were good, erosion was evident on the softer cored material, indicating the bit seal was likely no longer effective. It was also decided that the depth objective would not be attainable with the initial bit. Coring was therefore suspended with bit no. 1, an RBI CC-4 (SN BG255), at a depth of 2457.0 m (397.3 mbsf), and a free fall funnel (FFF) was deployed at 1515 hr, 28 January. The drill string was recovered and the bit reached the rig floor at 2100 hr that same day. The bit was found to be in poor condition with two cones extremely loose, two cones locked-up, and two jets plugged, although the cutting structure was undamaged. Evidence of bit balling and overload were evident, despite the high circulation rates (50-70 spm) used. Maximum weight on bit (WOB) had been 35,000 lb, although the majority of the coring was done with 25,000-30,000 lb WOB.

Because the cutting structure on the CC-4 core bit was in good condition but ROP was poor and bit balling was evident, an RBI CC-3 core bit (SN BG254) was selected for the next bit run. The RCB BHA was again run in the hole, and at 0315 hr, 29 January, after 15 min of camera scanning time, Hole 960A was reentered. The pipe was run to 2366.3 m (306.6 mbsf), and the top drive was then picked up. The pipe was washed/reamed to bottom within 1-1/2 hr, where 2 m of loose fill was evident. RCB coring resumed at 0700 hr, 29 January, and continued until 1630 hr, 30 January, when a depth of 2510.9 m (451.2 mbsf) was achieved. Recovery ranged from 18% to 65%. The ROP ranged from 1.7 to 3.2 m/hr.

After circulating a 30-bbl sepiolite mud pill, a wiper trip was made in preparation for logging. During the wiper trip, an overpull of 100,000 lb was experienced at a depth of 2488 m (approximately 428 mbsf). Another tight spot requiring 30,000 lb of overpull was identified between 2482 and 2453 m (DPM; 393-422 mbsf). As a result, the top drive was picked up and the hole was reamed from 2458 m (398 mbsf) to bottom. Eight meters of fill was encountered at the bottom of the hole. A second short wiper trip through the tight section of hole was then made to ensure good conditions for logging. No interference or drag was experienced during the second wiper trip. Two wireline runs were made to release the bit on-bottom and reverse shift the sleeve. A drift survey, taken on the last wireline run, indicated a hole deviation of 3.5° at total depth (TD). The lower 60 m of the hole was displaced with weighted mud, and the pipe was pulled to a logging depth of 2154.0 m (94.3 mbsf). At 0215 hr, 31 January, the logging sheaves were rigged and the quad combo geophysical suite of logging tools was run into the hole, but was unable to proceed farther than 2421.0 m (361 mbsf). Logs were attempted twice from this point up to 2135 m (75 mbsf); however, the calipers remained fully open throughout that interval, indicating that the hole was at least 17 in. in diameter. Based on this information, further logging attempts were abandoned.

Hydrocarbon indications were non-existent on this hole; however, the hole was filled with weighted mud, according to accepted guidelines, and the drill pipe pulled clear of the seafloor at

1245 hr, 31 January. After 1.5 hr was spent cutting and slipping the drill line, the pipe trip was resumed. The bit release reached the rig floor at 1700 hr, ending Hole 960A.

Hole 960B

The quality and recovery of the sediments recovered with the RCB coring system from the upper 200 mbsf of Hole 960A was poor, but theb sediments contained material of significant scientific value. It was thus decided to spud a second hole at this site using the APC/XCB coring system. In so doing, we were also hoping to determine if a PDC, drag-style, cutting structure on the bit would drill the formation at a more acceptable penetration rate than that achieved to date with the TCI roller cone bits. Hopefully, the recovery percentage and core quality would be improved as well. This information would be applicable to the drilling approach decided upon for the remaining two sites (Sites 961 and 962; proposed sites IG-2 and IG-3). An APC/XCB BHA was made up without a non-magnetic drill collar, as it had been decided that core orientation would not be attempted on this hole, in order to conserve the time for achieving a deeper penetration below the seafloor. The drilling assembly was terminated with a rebuilt 10-1/8-in. RBI XCB PDC bit (SN BC376). The bit had 22 rotating hr prior to this deployment. At 2245 hr, 31 January, after offsetting the vessel 100 m to the north, Hole 960B was spudded, and a single APC core recovering 7.13 m of mud-line sediment was taken. This established a mud-line depth of 2045.4 m (DPM). The corrected precision depth recorder reading normalized to driller's datum for this hole was 2047.4 m (PDR). A request from the curator at the Gulf Coast Repository for additional mud-line core material from this site resulted in Hole 960B being a single core hole only. Hole 960C, it was decided, would be taken to a greater depth. At 2245 hr, 31 January, Hole 960B was ended as the drill string was pulled clear of the mud line.

Hole 960C

After recovering Core 159-960B-1H, the APC was again run in the hole, and Hole 960C was spudded at 2330 hr, 31 January. Continuous APC coring continued into the following day, until Core 159-960C-16H indicated that an incomplete stroke was achieved. A total of 16 APC cores were taken, recovering 105.5% of the section. Coring with the APC was terminated at a depth of 2186.5 m DPM (140.2 mbsf). XCB coring resumed with Core 159-960C-17X, and by 1730 hr, 1 February, a cored depth of 2257.0 m DPM (210.7 mbsf) was attained. Recovery for the eight XCB cores taken was generally poor, ranging from 2% to 22%. At this time, the Co-Chief

Scientists agreed that the area of interest had been cored to a sufficient depth. Given time limitations for the remainder of the leg, it was decided to drill ahead with the XCB PDC bit and center bit to identify what ROP might be achievable. If a fast enough drilling rate could be sustained, the desire was to take Hole 960C to a total depth of 350-400 mbsf and attempt to recover the logging data (primarily FMS) that was not attained in Hole 960A.

Drilling proceeded for 16.75 hr, until a depth of 2379.5 m DPM (333.2 mbsf) was reached. For the first 6-7 hr of drilling, a penetration rate of 16 m/hr was achieved. This slowed to slightly fasterthan 10 m/hr for the final 10 hr. Two XCB cores (Cores 159-960C-25X and -26X) were cut at this point in an attempt to again core through the boundary of the A/B seismic units. After recovering these cores, drilling was resumed and continued to a depth of 2424.0 m, or 377.7 mbsf, where the ROP had slowed to 4.3 m/hr, so that the decision was made to terminate the hole. The hole was circulated with a 30-bbl sepiolite mud pill, and the center bit was recovered via sand line. During the final sand-line run, a multishot deviation survey was taken, indicating a hole drift of 2.5˚-3.0˚ at TD. A wiper trip up to 81.7 mbsf was made, with no indication of any hole problems. Approximately 1 m of fill was identified on bottom, which was reamed through and circulated out of the hole. At 0445 hr, 3 February, preparations for logging began. Since there was no interest on the part of the scientific party for anything other than FMS logs, and there was concern over hole deterioration with time, a request was made to LDEO for permission to make the FMS the first and only logging run. This was discouraged by LDEO, and it was decided to take the extra time required to run the quad combo tool string first. The nuclear source was left out to save a little time and minimize the risk of losing additional time should the tool be lost in the hole. During the first logging run, the tools stopped at 2170 m (123.7 mbsf) and the winch operator was unable to achieve any additional depth. The tool string was recovered and the drill pipe was lowered to 2215 m (168.7 mbsf) without incident. The quad combo tool string was again run into the hole and was able to get to within 4 m of hole TD (377.7 mbsf). Logs were obtained from this point up to drill-,pipe depth. Based on caliper data, it appeared that again much of the hole was washed out and eroded to at least 17 in. in diameter, despite the low flow rates (50 SPM max) used, and the relatively few hours the hole had been open and exposed. Next, the FMS logging tools were deployed reaching a depth of 2400 m or 24 m from TD. Upon conclusion of the logging program, the pipe was lowered to 2390 m and the hole was displaced with heavy mud. The pipe was pulled out of the hole, clearing the seafloor at 2215 hr, 3 February. The positioning beacon was released and recovered, with the bit reaching the rig floor at 0230 hr, 4 February, ending Hole 960C.

Results with the XCB PDC bit had been encouraging enough to consider deployment of the RCB PDC anti-whirl version on Site 961 (proposed site IG-2).

TRANSIT TO SITE 961
(Proposed site IG-2)

The vessel moved to Site 961 in DP mode while continuing to trip the drill string, following the bit clearing the seafloor at Site 960. Once the bottom hole assembly (BHA) components had beenracked back into the derrick, the rotary table was available for use in the disposal of 2520 m of sand line from the aft core winch. This cut was required to get beyond a portion of the line that had broken. Approximately 15 m of line on either side of the damaged section was retained for evaluation by the sand-line manufacturer. An RCB polycrystalline diamond compact (PDC) anti-whirl bit was made up to a mechanical bit release, and the RCB core barrels were spaced-out in the outer core barrel. The remainder of the RCB BHA was then made up, and the rig crew began tripping the drill string to the seafloor. Prior to reaching bottom with the drill string, at 0920 hr, 4 February, the signal from the pre-deployed positioning beacon was acquired and, by 1015 hr, the vessel was within 20 m of the site coordinates.

SITE 961
(Proposed site IG-2)

Hole 961A

After the drill pipe was run into the hole and the top drive was picked-up, Hole 961A was spudded at 1230 hr, 4 February. The mud line was established at 3303.6 m by DPM. The corrected PDR reading normalized to driller’s datum was 3302.4 m. RCB coring continued for the next 2-1/2 days
(35 cores), at which point a depth of 3612.3 mbrf, or 308.7 mbsf, was achieved. Recovery was extremely erratic, ranging from as little as 0% to as high as 56%. Overall, the recovery was a relatively poor 19.7%. The ROP with the RCB PDC anti-whirl bit was initially better than that achieved in similar formations with the CC-3 and CC-4 TCI core bits. ROP for the first day, 0-

126 mbsf, averaged 39.7 m/hr. By the second day, the sediment became noticeably stiffer and extremely sticky. The clay appeared to be water-sensitive, becoming very slippery when wet, yet retaining a hard, plastic property when compacted and dried by the drilling operation. The result was a severe problem with bit balling and bit-jet plugging. ROP on the second day had slowed to an average of 10.1 m/hr. Circulation flow rates were continually increased in an attempt to keep the bit from balling and the jets open, but to little, or no, avail. The ROP further deteriorated to an average of 4.1 m/hr on the third day, and the recovered core began to exhibit evidence of core erosion, likely due to a failed bit seal. Pump pressures indicated that at least half of the six bit jets were plugged, and the poor ROP confirmed a continued balling problem.

As a result of the core quality deterioration and poor ROP, it was decided that the bit should be pulled and inspected. An FFF was deployed, followed by the vibration-isolated television (VIT) frame. The mini-cone appeared to be in proper position on the seafloor as the bit came clear of the hole and was tripped to the surface. At 0930 hr, 7 February, the bit was at the rig floor. Upon inspection, it was found to be severely balled, three of six jets were plugged, and three external PDC gauge cutters were missing. All of the remaining PDC cutters appeared to be in excellent condition. Approximately one quarter of the bit body was worn in a 90° quadrant, where the outside diameter (OD) gauge cutters were missing. It would have been the preferred option to continue drilling with the bit, had it been re-runnable. The missing cutters were likely broken during the course of drilling through chert layers in the upper part of the hole. The ROP achieved with this bit was 2-4 times that achieved with the TCI bits. Since the bit was not re-runnable, it was decided that a cheaper CC-3 bit would be used next in order to avoid leaving an expensive new PDC bit in the hole. This bit would have to be dropped in the hole to allow logging, even though it would then have drilled only 300 m.

The BHA was made up, the core barrels were spaced-out, and the drill pipe was tripped back to bottom. At 1615 hr, after 15 min of vessel maneuvering, the FFF was reentered, and the pipe was run into the hole to 3568 m (264.4 mbsf), at which time the top drive was picked-up. While preparations for the resumption of coring operations were proceeding, the VIT frame was being recovered. However, at 1715 hr, 7 February, the coaxial cable parted with the VIT frame at 752 mbrf. The winch operator reported that he did not have the VIT frame weight after being informed by the DP operator that cable continuity had been lost and the breaker had tripped twice in succession. The top drive was then set-back again and the drill string was tripped back to the ship in the hope that the small diameter sleeve on the VIT frame survived the impact and the unit would come back riding on the bit body. The bit cleared the seafloor at 1830 hr, and at 2330 hr that same day, the VIT frame and 750 m of coaxial cable arrived in the moon pool. During this trip, discussions were held convering various drilling options. It was decided that the best course of action was to spud a new hole rather than wait on the status report and subsequent repairs to the TV reentry system. The remaining coaxial cable had been inspected to a depth of 4700 m and was found still to be of questionable integrity, due to extremely corroded and brittle armor wires. Re-heading the cable at that point was considered imprudent and would take up to 24 hr. To set-up and spool on the spare coaxial cable, stored in the riser hold, was estimated to take upward of an additional 12 hr. It was unknown what damage, if any, may have been sustained by the VIT frame itself or the TV/sonar electronics mounted on it. Hole 961A was considered officially terminated at 2330 hr, 7 February, the time at which the bit/VIT frame arrived at the moon pool.

Hole 961B

A total of 2 hr was expended cutting away, and untangling, the 750 m of failed coaxial cable piled on top of, and beneath, the VIT frame. The failed wire was disposed of and the ship was offset 100 m west in preparation for spudding the next hole, assuming that the sediment layer would be thinner as we moved updip, up the slope of the Marginal Ridge. Once the VIT frame was cleared and removed, the same drill pipe and RCB BHA from Hole 961A were tripped back to the seafloor. Hole 961B was spudded at 0800 hr, 8 February. Since the PDR depth was virtually the same as the previous hole, the same water depth of 3303.6 m (DPM) was used. RCB coring was initiated at a depth of 3519.9 m (216.3 mbsf) after drilling down with a center bit at an average ROP of 23.0 m/hr. A total of four spot cores were taken, alternating with occasional center bit drilling, to a depth of 3571.1 m or 267.5 mbsf. The cores were taken periodically because, rather surprisingly, the net ROP with a core barrel in place seemed to be better than that achieved with the center bit, even with allowances for the additional wireline time required.

Continuous RCB coring was initiated with Core 159-961B-5R and continued to a depth of 3673.5 m (369.9 mbsf) before deteriorating hole problems prompted remedial action. Recovery over this interval was quite erratic due to the alternating hard and soft interbedded sediments and scattered chert layers. The average daily recovery ranged from 20% to 60%. Likewise, the ROP varied greatly, ranging from 1.5 to 10.5 m/hr. Bit balling probably caused some of the poor drilling rate problems. Drilling parameters varied extensively, all with little, or no, effect on recovery and/or ROP. Coring was terminated at a depth of 369.9 mbsf, when high pump pressures and torquing indicated hole instability. The pipe was worked off bottom and the hole was back-reamed to a depth of 206.7 mbsf. At that point, a 20 bbl-high viscosity mud pill was circulated and the pipe was advanced back to bottom with normal pressure and torque parameters. A total of 7 m of fill, found on bottom, was washed and reamed out of the hole, and another mud pill was circulated downhole. After recovering the core barrel, hole conditions remained favorable and coring resumed at 2030 hr, 11 February 1995. Coring continued with Core 159-962B-19R to 3678.2 m (374.6 mbsf); however, hole instability again became a problem, and it soon became apparent that continued attempts to deepen the hole were futile. Coring was abandoned at midnight that night, and preparations were begun to pull out of the hole. The drill pipe was pulled clear of the seafloor at 0130 hr, 12 February. The top drive was racked back and the pipe trip continued. While recovering the remaining drill string, the positioning beacon was released and recovered, and the vessel began moving in DP mode to the Site 962 (proposed site IG-3) operating area. At 0715 hr, 12 February, the bit cleared the rig floor, ending Hole 961B.

TRANSIT TO SITE 962
(Proposed site IG-3)

While en route to Site 962, the rotary bit, mechanical bit release, and RCB were laid out, and the drilling line was cut and slipped. The rig crew then started to make-up the APC/XCB BHA. In addition to spacing out the APC/XCB core barrels, the Motor Driven Core Barrel (MDCB) was function tested at the rig floor. The tool failed to unlatch during the pumping test. Upon inspection, it was determined that the latching mechanism and thruster shaft had seized up, probably due to several months' storage in the core barrel storage shucks. After freeing-up these components, the tool was again tested. This time unlatching and proper rotation were verified. The tool was then set aside and the remaining portion of the BHA was assembled. At 1015 hr, 12 February, the vessel was within 0.9 mi of the site coordinates, at which time the pre-placed positioning beacon was commanded on and the acoustic signal acquired. By 1130 hr, the vessel was positioning in automatic mode over Site 962.

SITE 962

Hole 962A

The drill string was tripped to the seafloor, where the top drive was picked-up, and the APC core barrel was deployed. The corrected PDR reading normalized to driller's datum for this hole was 4621.4 m. Coring began with a request for one additional mud-line core. In an attempt to maximize recovery for sampling purposes, the first APC was taken from a depth of 4619 m. Three water cores in succession followed until 3.71 m of core was recovered, establishing the seafloor at a depth of 4648.9 m by DPM. Hole 962A was spudded at 2330 hr, 12 February, after which the APC was immediately retrieved, thus ending Hole 962A after a single piston core.

The relatively large depth discrepancy between PDR and drill-pipe measurement was never accounted for. A check of the pipe tally revealed no errors or "missing" stands. Likewise, another check of the PDR system resulted in identical results as the initial reading.

Hole 962B

After recovering the only core taken from Hole 962A, the APC core barrel was again run to bottom and Hole 962B was spudded at 0045 hr, 13 February, with water depth for this hole being established at 4648.7 m (DPM). Continuous APC coring continued until reaching a depth of 93.3 mbsf (Core 159-962B-11H). Core orientation using the Tensor tool was attempted in this hole, starting with Core 159-962B-3H. Coring continued without problems until Core 159-962B-10H, which did not fully stroke and required 100,000 lb to pull free. On retrieval of the core barrel, a few pieces of chert were found in the liner. The final APC core of Hole 962B (Core 159-962B-11H) also did not exhibit normal end-of-stroke pressure bleed-off; however, it required only 30,000 lb to extract it from the formation. Upon recovery, the barrel again had just a few pieces of chert in the core catcher. As a result of these coring difficulties, coring proceeded with the XCB for the next two cores (Cores 159-962B-12X and -13X) to a depth of 4748.7 m (DPM) or 100.0 mbsf. The drilling of this interval was characterized by abnormally high pump pressure (40 spm, 1200 psi) and high torque (500-700 amps). Little progress was made before the ability to circulate was completely lost and the pipe became stuck. Within 30 min, circulation was again established and the string was freed with 150,000 lb of overpull. As a result of these problems, a 20-bbl high-viscosity mud pill of Bentonite gel was circulated, and the core barrel was recovered. A center bit was dropped, and efforts were continued to clean-up and stabilize the hole. At 2230 hr, after advancing to a total depth of 4752.4 m (103.7 mbsf), the hole was abandoned due to continued and worsening hole conditions. The drill string was pulled out of the hole, clearing the seafloor at 2300 hr, 13 February. The top drive was set-back, and the drill string was tripped back to the vessel. The bit reached the rig floor at 0730 hr, 14 February, ending Hole 962B.

Hole 962C

While the BHA was changed over from APC/XCB to an RCB configuration, the ship was offset 50 m to the west. The drill pipe was tripped to the seafloor, and Hole 962C was spudded at 1630 hr, 14 February. With a center bit in place, the bit was advanced to a depth of 4712.3 m (73.0 mbsf), where continuous RCB coring commenced. Hole trouble was apparent from the onset of coring operations. Core 159-962C-1R advanced to a depth of 82.6 mbsf; however, after picking up a single stand of pipe, the hole was found to have 1 m of fill on-bottom. While attempting to cut Core 159-962C-2R, high torque and pump pressure were evident. After working the pipe around in the hole for a while, Core 159-962C-2R was eventually cut to a depth of 92.3 mbsf. Despite circulating a high viscosity mud pill in an attempt to clean-up the hole, conditions did not improve. Continued working of the pipe was unsuccessful and it became more and more difficult to reach the bottom of the previously drilled hole. At 0200 hr, 15 February, Core 159-962C-2R was recovered, and another barrel was pumped to bottom. However, on lowering the pipe, another 3 m of fill was found at the bottom of the hole. Attempts to advance through the fill resulted in high torque and continued sticking of the pipe. A sepiolite mud pill was circulated in the hope that the superior viscosity would aid in hole cleaning. However, all efforts to reach the original bottom of the hole were frustrated by the hard, broken, chert-like formation. The decision to abandon the hole was made at 1200 hr, 15 February. After the core barrel was recovered, the drill pipe was pulled clear of the seafloor at 1300 hr, 15 February, ending Hole 962C.

Hole 962D

One final attempt to achieve deep penetration and coring was made at Hole 962D. It was decided that, should the same unstable hole/drilling conditions appear in this hole, operations at this site would be abandoned in favor of drilling at the proposed alternate site IG-2C, close to Site 961.

The ship was offset 100 m east in the hope that drilling conditions would be improved. At 1330 hr,
15 February, Hole 962D was spudded, establishing a seafloor depth of 4657.0 m (DPM). The corrected PDR reading normalized to driller's datum for this hole was 4623.8 m. With a center bit in place, the bit was advanced to a depth of 4732.1 m (75.1 mbsf), where continuous RCB coring commenced. Continuous RCB coring (Cores 159-962D-1R to -19R) continued to a depth of 4913.4 m (256.4 mbsf). Recovery in this interval was highly variable, ranging from 0 to 85%. The rate of penetration was also quite erratic, varying from 5.7 to 12.8 m/hr.

GC3 and NGA analysis on Core 159-962D-9R, immediately below the chert layer, indicated the first presence of long-chain hydrocarbons, which ranged as high as C_5. Core 159-962D-13R contained 6 ppm of NC6, although this proved to be the only occurrence of this hydrocarbon in Hole 962D. As coring progressed, the percentage of hydrocarbons decreased downhole, except for occasional spikes related to shale interbeds with high organic content. The highest concentration of Methane (C_1; 10%) occurred in Core 159-962D-28R. No predictable trends were noted downhole.

While cutting Core 159-962D-19R, the top drive swivel began leaking hydraulic oil. After recovering Core 159-962D-19R at 1130 hr, the top drive was set back, the drill pipe was pulled to a depth of 4751.4 m (94.4 mbsf), and the circulating head was installed. A constant drag (overpull of 35,000-40,000 lb) was experienced in the lower 60 m of Hole 962D. Once above that point, the hole appeared to be in good condition to 133 mbsf, where the same tight spot seen on the previous wiper trip was encountered.

Work then commenced on the replacement of the power swivel with the spare unit that had been stored in the riser hold. By 1800 hr, 17 February, the spare swivel had been installed, the wireline blowout preventer (BOP) and WKM valves reinstalled, and all hoses reconnected. The drill string was run back into the hole to 4847.0 m (190.0 mbsf) and the top drive was picked-up. The last 66 m of hole required washing and reaming until the original depth of 4913.4 m (256.4 mbsf) was reached. A 15-bbl sepiolite mud pill was circulated and, at 2230 hr, the drilling center bit was recovered.

Continuous RCB coring resumed with Core 159-962D-20R and continued until Core 159-962D-30R was recovered from a depth of 5002.3 m (345.3 mbsf). However, as coring for this core was about to be completed, the hole suddenly collapsed and the drill pipe became stuck. All attempts to circulate and/or rotate were unsuccessful. The pipe was worked until eventually the pipe could be moved downhole. Top-drive rotation was then established, but the hole was still packed-off around the drill string. After 1.25 hr, and overpulls of up to 100,000 lb, the pipe was freed. After recovering Core 159-962D-30R, it was decided to make a wiper trip to check conditions over the remaining portion of the hole. The top drive was set back and the drill string was pulled to a depth of 4760.0 m (103.0 mbsf). A continuous drag of 20,000-30,000 lb, with a maximum of 60,000 lb, was noted during the wiper trip. The pipe was run back into the hole to a depth of 4944.0 m (287.0 mbsf), where the top drive was picked-up. The remaining portion of the hole was washed and reamed until the original TD of 5002.3 m (345.3 mbsf) was reached. A total of 2.0 m of fill was found at the bottom of the hole. At 1400 hr, 19 February, continuous RCB coring was again initiated and continued until 1645 hr, 20 February, when the final depth of the hole was achieved at 5050.5 mbrf (393.5 mbsf). Coring was terminated to allow adequate time for logging the hole prior to abandonment.

Logging Operations

The top drive was set back and another “pre-logging” wiper trip with the drill pipe was again made to 4760.0 mbrf (103.0 mbsf). As experienced earlier, there was moderate drag throughout the wiper trip, which reached a maximum of 80,000 lb overpull at one point. The drill pipe was run back in the hole and the top drive picked-up at a depth of 4992.0 mbrf (335.0 mbsf). After reaming the lower portion of the hole to TD, a 30-bbl sepiolite mud pill was circulated from the bottom up, and two successive wireline runs were made to release the bit and reverse shift the sleeve. The drill pipe was then pulled to a logging depth of 4789.7 mbrf (132.7 mbsf). This depth was selected to put the drill pipe across the zone where excessive overpull had been experienced on the two previous wiper trips.

The first logging run was made with a reduced geophysical logging string comprising the phasor dual induction resistivity tool (DIT), lithodensity logging tool (HLDT), sonic digital logging tool (SDT), and the NGT. The nuclear source was left out to eliminate any chance of loss in the hole and potential associated problems. This run was aborted when the tools would not pass 4809.0 mbrf (152.0 mbsf). The pipe was lowered to a depth of 4848.0 m (191.0 mbsf), using the circulating head, and the logging run was repeated. The tools reached a depth of 4988.0 mbrf (331.0 mbsf), within 62.5 m of bottom. Logging proceeded from that depth back to the drill pipe and was repeated before recovering the logging tools. Prior to running into the hole with the FMS tool, the drill pipe was lowered an additional stand to 4876.6 m (219.6 mbsf), placing it across an area of bad hole conditions at 4868.0 mbrf or 211.0 mbsf. This was done to increase the chances that the FMS tool would reach the deeper, more scientifically interesting, part of the hole. The FMS tool reached a depth of 4948.0 mbrf (291.0 mbsf). Two runs were made from that depth back to the end of the drill pipe. On all logging runs, the drill pipe was raised an additional 20 m as the logging tools approached the end of their run.

While the FMS logging tools and sheaves were being rigged down, the circulating head was installed and Hole 962D was displaced with heavy mud. The drill string was pulled out of the hole, clearing the seafloor at 2400 hr, 21 February. At this point, the aft (short) sand line was run into the pipe and coated with preservative. The positioning beacon was released and recovered. The drill string was tripped back to the rig floor and the drill collars/subs were magnafluxed, during which time the damaged coaxial TV cable was disposed of in preparation for installation of the new line during the Marseille port call. While the pre-transit work was being completed, the thrusters were raised, and the ship was secured for the 2117 nmi voyage to Las Palmas, Canary Islands. At 1430 hr, 22 February, the vessel got under way for port.

The first line ashore at Las Palmas was at 0700 hr, 2 March 1995, officially ending Leg 159.

OPERATIONS SUMMARY

Leg 159

	Days
Total Days (3 January 1995 - 2 March 1995)	58.00
Total Days in Port 1.31	
Total Days Underway	12.77
Total Days on Site	43.92

	Days
Coring	26.88
Repair Time (Contractor)	0.34
Tripping	7.28
Reentry	0.07
Logging/Downhole Science	3.98
Drilling	2.75
Other	2.23
Stuck Pipe/Downhole Trouble	0.39
Fishing & Remedial	0.00
Casing & Cementing	0.00
Development Engineering	0.00
W.O.W.	0.00
Repair Time (ODP)	0.00

Total Distance Traveled (nmi)	3521.5
Total Miles Transited	3380.5
Average Speed Transit (kt)	11.9
Total Miles Survey	141.0
Average Speed Survey (kt)	6.5
Number of Sites	4
Number of Holes	13
Total Interval Cored (m)	3167.4
Total Core Recovered (m)	1878.0
% Core Recovery	59.3
Total Interval Drilled (m)	955.1
Total Penetration (m)	4122.5
Maximum Penetration (m)	1158.9
Maximum Water Depth (m from drilling datum)	4657.0
Minimum Water Depth (m from drilling datum)	2101.2
Reentries	2

SITE SUMMARY

Leg 159

HOLE	LATITUDE	LONGITUDE	WATER DEPTH (mbrf)	NUMBER OF CORES	INTERVAL CORED (m)	CORE RECOVERED (m)	PERCENT RECOVERY (%)	DRILLED (m)	TOTAL PENETRATION (m)	TIME ON HOLE (hr)	TIME ON SITE (days)
959A	03°37.659'N	02°44.112'W	2102.0	52	480.7	456.21	94.9	0.0	480.7	67.75	2.82
959B	03°37.657'N	02°44.135'W	2101.5	20	184.4	192.53	104.4	0.0	184.4	15.00	0.63
959C	03°37.669'N	02°44.116'W	2101.2	20	179.6	187.34	104.3	0.0	179.6	20.75	0.86
959D	03°37.656'N	02°44.149'W	2102.0	78	741.1	429.03	57.9	417.8	1158.9	245.50	10.23
TOTAL - Site 959 (proposed site IG-1)				**170**	**1585.8**	**1265.11**	**79.8**	**417.8**	**2003.6**	**349.00**	**14.54**
960A	03°34.977'N	02°44.009'W	2059.7	61	451.2	145.00	32.1	0.0	451.2	179.50	7.48
960B	03°35.024'N	02°43.986'W	2045.4	1	7.1	7.15	100.7	0.0	7.1	5.75	0.24
960C	03°35.025'N	02°43.990'W	2046.3	26	230.3	160.80	69.8	147.4	377.7	75.75	3.16
TOTAL - Site 960 (proposed site IG-1bis)				**88**	**688.6**	**312.95**	**45.4**	**147.4**	**836.0**	**261.00**	**10.88**
961A	03°26.542'N	03°03.513'W	3303.6	35	308.7	60.42	19.6	0.0	308.7	93.00	3.88
961B	03°26.556'N	03°03.560'W	3303.6	19	134.8	56.74	42.1	239.8	374.6	103.75	4.32
TOTAL - Site 961 (proposed site IG-2)				**54**	**443.5**	**117.16**	**26.4**	**239.8**	**683.3**	**196.75**	**8.20**
962A	03°15.077'N	03°10.921'W	4648.9	1	3.7	3.71	100.3	0.0	3.7	16.25	0.68
962B	03°15.063'N	03°10.919'W	4648.7	13	100.0	85.60	85.6	0.0	100.0	32.00	1.33
962C	03°15.057'N	03°10.943'W	4639.3	3	29.4	0.51	1.7	73.0	102.4	29.50	1.23
962D	03°15.082'N	03°10.898'W	4657.0	37	316.4	92.76	29.3	77.1	393.5	169.50	7.06
TOTAL - Site 962 (proposed site IG-3)				**54**	**449.5**	**182.58**	**40.6**	**150.1**	**599.6**	**247.25**	**10.30**
LEG 159 TOTALS -				**366**	**3167.4**	**1877.80**	**59.3**	**955.1**	**4122.5**	**1054.00**	**43.92**

Site Summary-See Table 1 (Excel)

Leg 159 - Total Time Distribution

2.1 Days in Port (4%)
12.3 Days Underway (24%)
37.3 Days On-Site (72%)

TECHNICAL REPORT

The ODP Technical and Logistics personnel aboard *JOIDES Resolution* for Leg 159 were:

Laboratory Officer:	Burney Hamlin
Marine Laboratory Specialist (Photography):	Roy Davis
Marine Laboratory Specialist:	Paul Davis
Marine Laboratory Specialist (Storekeeper):	John Dyke
Marine Laboratory Specialist (Paleomagnetics):	Edwin Garrett
Assistant Laboratory Officer (U/W Lab):	Dennis Graham
Marine Laboratory Specialist (Thin Section):	“Gus” Gustafson
Marine Laboratory Specialist (Yeoperson):	Michiko Hitchcox
Marine Laboratory Specialist (Physical Properties):	Taku Kimura
Marine Computer Specialist:	Terry Klepac
Marine Computer Specialist:	Matt Mefferd
Marine Electronics Specialist:	Eric Meissner
Marine Electronics Specialist	Dwight Mossman
Marine Laboratory Specialist (Chemistry):	Chieh Peng
Marine Laboratory Specialist (Chemistry):	Phil Rumford
Marine Laboratory Specialist (X-ray):	Don Sims
Marine Laboratory Specialist (Curatorial):	Lorraine Southey

PORT CALL

The technical staff and scientists began arriving in Paris’s Charles de Gaulle Airport for the flight to Dakar, Senegal, on 2 January 1995. The flight arrived late that evening, and we were accommodated at the hotel by midnight. The following day we were taken by bus to the ship for an abbreviated port call. Crossover with the transit personnel was brief, as little beyond immediate post-dry dock work had been accomplished during the transit from Falmouth, United Kingdom. Offices had been returned to normal, and all stored equipment and computers were put back into service. No shipments to, or from, Dakar were necessary, as the ship had received freight, provisions, and bunker in Falmouth. Other scientists and SEDCO personnel arrived 3 January.

TRANSIT TO OPERATING AREA

Watches were assumed within hours of the departure of *JOIDES Resolution* from port. The newly installed PELAGOS Real Time Navigation (RTN) system and software was put into service. The 5-day transit to the selected drilling sites provided an opportunity for the underway specialist and electronics technicians to become familiar with the software and to explore its features. The transit to the drilling sites off the shore of Côte d'Ivoire and Ghana was routine. Speeds in excess of 14 kt were logged, gaining time which was used for a seismic survey over all three of the primary drilling sites together.

The Co-Chief Scientists designed a 30 hr survey and specified two 200-in^3 water guns to provide maximum penetration through the thick sedimentary layer. Waypoints were selected, and preferred survey patterns were graphically presented on the bridge.

Signals from the starboard hydrographic array were noisy, in spite of the normal records collected the week before when a test drill site on the transit to Dakar was surveyed. The electronics specialist opted to trouble-shoot the dead port streamer and found that the winch side of the slip ring wiring had failed. Jumpers provided a signal from the streamer, but it too was noisy. The seismic records that were collected proved usable and, when processed, were comparable to previous records. The survey of the last site was abbreviated, as the record gave no surprises in the

light of the pre-cruise surveys, and the seismic gear was retrieved at 0630 hr, 9 January. The ship was positioned and activities began with APC coring at Site 959.

As the drill sites were only tens of miles apart, the ship was maneuvered from site to site in DP mode with the positioning hydrophones up. Track lines were graphically presented between sites which were overlaid by the ship's track.

Site activities were terminated by 1430 hr, 22 February. Navigation and magnetic information was collected on the transit to Las Palmas, Gran Canaria.

CURATION

A wide range of materials was recovered, ranging from pelagic muds to cherts, shales, siltstones, and sandstones. Gassy zones resulted in pressure forcing core caps off the capped core sections. The high-resolution samples taken during Leg 159 were primarily from the triple APC Hole 959C. Sampling these cores was complicated, as there were far more shore samples approved than usual, raising the topic of formally deferring some of the shore-based requests to the repositories, where the samples would then be taken when a sampling strategy could be worked out with the ship's preliminary results. The extra shipboard samples can represent a lot of work, and the material is also depleted before the shipboard scientists have formulated the most effective sampling strategy.

Other sampling problems were related to the taking of slabs, whole rounds, and to the size of the samples scientists requested. Limits, waivers, advice, and further justifications were needed to guide the sampling effort.

Cores taken on the transit from Falmouth to Dakar (Site 958) were included in the refrigerated container being sent to the Gulf Coast Repository. Cores collected from the Leg 159 drill sites were sent to the Bremen Core Repository. A large frozen shipment of samples was sent to the University of Bremen.

CORE LABORATORY

Laser Particle Counter

The older SPECTREX model was replaced by a new particle counter, a SPECTREX PC-2000. The new unit is easier to use and has a better data display. While the new instrument is more accurate over a wider range of standards, including clays, there were problems encountered during this leg when clays were missed in the sediments. The company has been made aware of our problem, and advice has been received to remedy the difficulty . A satisfactory result is anticipated.

PALEOMAGNETICS LABORATORY

Cryogenic Magnetometer

The cores recovered during Leg 159 possessed very weak magnetic signatures, which necessitated many tests and fine tuning sessions to verify that the cryogenic magnetometer was functioning as designed. A suggestion was made to standardize the laboratory equipment and programs to ODP-preferred units and to relabel the equipment. However, the problem is more detailed and the topic will be discussed with the responsible Laboratory Working Group (LWG). The Tensor tool was used to orient the APC recovery on several holes, but the value of the data was diminished by the weakness of the sediment magnetic signatures. Two other topics for LWG discussion are ways to make the Tensor tool output directly usable and to improve the VAX orientation program. The current steps needed for both operations are too involved and time consuming. A graph printing sequence was streamlined to allow quick prints and easy modification of graphs.

PHYSICAL PROPERTIES LABORATORY

MST

Previous problems with the MST have rarely occurred since the introduction of a more robust drive belt and some automated features. Delays were few, and, with routine adjustments, the 1565 sections measured moved smoothly through the laboratory. All other routine physical properties measurements were made, including resistivity, index properties, velocity measurements, and shear strength values. A report documenting the area of influence around the magnetic susceptibility meter on the MST was made and sent to shore. Updating of the physical properties manual to increase ease of use was commenced.

CHEMISTRY LABORATORY

Nearly all of the suite of instruments available in the chemistry laboratory were used to support the interstitial water determinations and organic chemistry. The natural gas analyzer and gas chromatograph #3 supporting headspace gas analysis were heavily used and supported the gas safety program as required. The Rock-Eval instrument reported carbon maturity in the samples, and the coulometer defined the carbonate ranges. The coulometer light sensor was replaced with one borrowed from the backup unit. Prior to the first site, the Dionex titrator was repaired with a temporary power transformer, and the unit performed well. Some heavier hydrocarbon gases (propane through hexane) were detected, raising safety issues; however, they were found in trace amounts only.

X-RAY LABORATORY

Few problems were encountered in preparing over 500 XRD samples for analysis, almost exclusively for clay mineralogy. Centrifugal and simple separation samples were vacuum filtered, glyconated as needed, and analyzed. Some difficulty was noted in keeping order in the files, as the samples were received from different sites and holes at different times. Three sediment samples were taken for X-ray fluorescence (XRF) trace element analysis, two of which were rich in barium and were outside the calibration curves. During this leg, space was not available in the paleontology preparation area for X-ray sample preparation. Vacuum filtering the samples in the X-ray preparation area precluded other uses in the area.

PALEONTOLOGICAL LABORATORY

This laboratory was used heavily during the leg and functioned smoothly. One set of palynology samples was prepared through a barren zone. The FossiList Program caused some difficulties, and was abandoned after data were lost. The program crashed because it was being backed up by incompatible software (Retrospect), and when this problem was alleviated, the FossiList program was again used during the last two weeks of the cruise.

COMPUTER SERVICES

Those computers and parts of the network that were affected by the removal of asbestos ceiling panels in the ship house were reinstalled during the transit to Dakar and were received in ready-to-use condition. Two major hard drive failures occurred once the ship was on site. One VAX 1GB drive dropped off line, and a week later the internal component began logging errors once blocks of data began moving over the network. There were also problems with the UserVolume drive. Smaller hard drive replacements and reassignments were made, resulting in a recommendation that several 1 GB hard drives be purchased as a new suite of primary hard drives. Replacements and hardware fixes are expected in port.

Otherwise, the VAX system worked well, though the limits of some of the older computers have been reached, primarily the Mac 11x's, Si's, and the older PC's. New versions of programs are large and run very sluggishly on these old machines. Scanners and optical character reading (OCR) software, coupled with CD-ROM drives attached to these limited systems, result in regular crashes and poor performance. The SUN in the user room was little used.

Problems relating to the shipboard implementation of beta software developed. Feedback of the various FossiList problems to the shore programmer was not as timely, or as complete, as needed to advance the program during this leg. As valuable as the programs may be, the system managers have not yet had the opportunity to invest adequate time into expeditiously evaluating problems or fixing errors. Nor are they skilled enough users to teach and support the program for new users. New users do not have the patience or time to work through slow and flawed programs. Easing these programs into routine use will require on-board initiative and familiarity by the staff representative supporting the program in addition to the programmer’s experience of the package as it functions in a shipboard multiuser environment.

A PC was configured to run the RTN WinFrog software on the bridge, and the software was installed on a PC in the DP room. Written permission to set up another PC platform for this program in DP is being sought. Space considerations in the area will also be addressed. The data on WORM media were inventoried, and the request to convert the data from our WORM drive system to DAT tape was initiated. This backup session can take 12 hr and is sometimes terminated by tape errors. The effort will be continued. The new storage furniture in, and rearrangement of, the computer machine room contributes to a sense of organization and better space utilization.

A new computer system manager, Terry Klepac, was introduced to the computer systems and network and laboratory equipment.

MICROSCOPES AND PHOTOGRAPHY LABORATORY

The microscopes were cleaned and tailored to the scientists’ needs on the transit to the first site. A damaged objective and a poorly functioning centering stage were taken out of service. Attention was given to the microscope equipment, which was listed as missing during the dry-dock inventory check. A problem list was prepared for the Zeiss representative, who is scheduled to service the microscopes in Marseille.

The new photography distribution policy, sent out on Leg 158, was implemented without problems. The new policy reduces the number of prints required of the photographer and makes wider use of the prints that are made. Processor maintenance and cleaning were preformed. Fuji color chemistry was used, and concentrations were refined for optimum transparency quality. Photo assignments included documenting the National swivel failure, space layout in the downhole measurements laboratory and subsea shop, and a damaged subsea TV cable.

ELECTRONICS SUPPORT

Most of the problems deferred to the electronics specialists were minor, with the exception of the failure of a component in the XRF high-voltage power supply. Xerox copier maintenance and support were made on a daily basis at the main deck station until a series of major components were changed out. On site, slip-rings on the hydrographic winches were replaced or cleaned, and components and connectors were checked to the recorders. Underwater connectors in the streamer arrays were cleaned during the transit to Las Palmas. A streamer stretch section was taken out of

service to be refurbished ashore. Adara heat flow measurement support was given. Some maintenance was done on the TOTCO system, but indications are that this system will no longer be supported.

STOREKEEPING

Spot counts were conducted in the storage area as irregularities were found. Two containers of supplies originating at ODP were forwarded to the BCR with the core shipment. Future shipments to the BCR from the GCR should be handled by the storekeeper ashore to ensure that all the property numbers, quantities, and country of origin are supplied.

SPECIAL PROJECTS

A safety shower was installed at the upper ’tween landing adjacent to the Electronics Shop entrance. This location was convenient due to the presence of a potable water supply, a limited drain, and a well-lighted position about halfway between the elevator and the chemical storage lockers. The location was inspected after a SEDCO safety meeting and endorsed.

A request was made to SEDCO to drain the oil from the crane over the gym. Oil has leaked onto the gym equipment and was damaging the new flooring. The drilling superintendent concurred, and the unit was drained. PVC sheeting was taped up around it to catch the final drops of hydraulic fluid.

SAFETY

The METS team participated in the weekly boat and fire drills. A new safety video, *HearSafe*, was added to the ODP collection. The ground fault interruption (GFI) receptacles in the splitting room were tested, and GFI protection was added to the power strip serving the drill presses and saws in the sampling area.

LEG 159 LABORATORY STATISTICS

General	Sites:	4
	Holes:	13
	Meters Drilled:	955.1
	Meters Cored:	3167.4
	Meters Recovered:	1877.98
	Time on Site (days):	43.9
	Number of Cores:	366
	Number of Samples:	13,569
	Number of Core Boxes:	287
Downhole Tools	Adara HF:	7
Analysis	Magnetics Laboratory	
	Half section measurements:	2300
	Discrete measurements:	400
	Physical Properties	
	Index properties:	623
	Velocity:	1531
	Resistivity:	380
	Thermal conductivity:	261
	MST:	1565
	Shear Strength:	248
	Chemistry Laboratory	
	Inorganic Carbonates ($CaCO_3$):	561
	Water Chemistry (the suite includes pH, Alkalinity, Sulfate, Calcium, Magnesium, Chlorinity, Potassium, Silica, Lithium):	59
	Headspace gas analysis:	294
	Pyrolysis Evaluation:	
	Rock-Eval	104
	X-Ray Laboratory	
	XRD:	529
	XRF:	3
	Thin Sections:	100
Underway Geophysics (estimated)		
	Total Transit nmi:	3342
	Bathymetry:	2900
	Magnetics:	2756
	XBT's Used:	43